

Simulation Based Biarticular and Monoarticular Exoskeletons Design, Analysis, and Comparison

Ali KhalilianMotamed Bonab^{1*}, Volkan Patoglu¹

1 Human Machine Interaction Laboratory, Mechatronics Engineering, Faculty of Engineering and Natural Science, Sabanci University, Istanbul, Turkey.

* alik/vpatoglu@sabanciuniv.edu

Abstract

Introduction

The versatility and bipedalism of human locomotion are both unique [1] and the most important characteristics of humans among the mammalian mobility types. While bipedal locomotion has a low energy cost of transport [1], the human versatile musculoskeletal system is not perfectly appropriate for performing all the tasks [2]. For instance, among all movement tasks, two important tasks for human locomotion are running and walking, and it has been proven that running is considerably less efficient than walking [3, 4].

Bipedal locomotion can also lose its efficiency through aging, disease and injury, which can profoundly affect the quality of life [5] due to a loss of independence and mobility. It has been shown that static and dynamic strength [6–8], force development rate [9, 10], prolongation of twitch contraction [7, 11], and passive stiffness [12, 13] of the healthy elderly people's muscles have been remarkably changed compared to those of young, healthy people and consequence of these changes is the weakening the performance of gait [14].

Along with aging, disease and injury are other primary causes of inefficient human locomotion . One of the most important injuries is spinal cord injuries (SCI), which considerably affect the human ability to perform movement tasks [15]. Among all possible diseases causing gait variability, a hemiparetic walking is one of the most and major issues patients face after stroke [16–19]. A stroke can have a serious effect on motor cells and pathways of the central nervous system [17] which can remain after stroke for a long time, restricting patients from reaching normal speed, safe and economical gait [20]; leading to inability on generating desired muscle contraction [17], and generally impaired muscular control [21]. Loss of muscle strength [22], reduced ankle dorsiflexion, and knee flexion [23, 24] are some typical effects of stoke leading to a high cost of transportation on the patient.

Even though in the long term, training can improve the efficiency of locomotion [25] by increasing the stiffness of the tendons [26], and rehabilitation can help patients to achieve near-normal locomotion [20],the muscle and tendon tissues fundamentally constrain the dynamic properties of the muscles and musculoskeletal system compromises between enhancing the efficiency of the desired task and its adaptability [2], and persistence of the neuromotor deficits even after the rehabilitation constrains [20] the patients from completely resolving the gait issues and reaching complete independence.

By taking advantage of assistive devices not bounded by any fundamental biological limitations, a musculotendon system can be customized to increase the efficiency of performing the desired task while degrading versatility. It can be used for patients to improve their quality of life by modifying their abnormal gait pattern and decreasing their dependency; assistive devices can also be employed to reduce the risk of injuries for tasks needed to carry heavy loads [27–29].

Lower Limb Exoskeletons

The first efforts to develop mobile powered exoskeletons were initiated in 1890 [30]. Despite efforts and progress in accomplishing untethered exoskeleton over a century [31], in 2000 Defense Advanced Research Projects Agency (DARPA) initiated the Exoskeletons for Human Performance Augmentation (EHPA) Program [32], and the first mobile and functional exoskeleton, named Berkeley Lower Extremity Exoskeleton (BLEEX) was developed to augment soldiers' capability of carrying heavy loads over long distances [33]. Sarcos and MIT exoskeletons were introduced [30] after BLEEX as untethered exoskeletons. The same technology with the purpose of assisting impaired populations also was already initiated [34], and ReWalk is one of the well-known exoskeletons [35] which has recently been approved by FDA [36]. The Hybrid Assistive Limbs (HAL) project [37] is another notable project assisting SCI, stroke, and other patients suffering from impaired bipedal walking. Reviews on exoskeletons, prostheses, and orthoses are available in the literature [31, 36–39].

The main objective of assistive devices is reducing the metabolic cost of locomotion and, in particular, decreasing the metabolic energy required for running and walking tasks. Although efforts on designing active exoskeletons to reach this goal were initiated decades ago, the researchers have only recently succeeded in accomplishing this goal [40], which was a tethered device assisting ankle and $6 \pm 2\%$ metabolic cost reduction was reportedly achieved by the ankle exoskeleton. After this exoskeleton, Mooney et al. [41] and Collins et al. [42] reported the reduction of metabolic energy consumption using their ankle exoskeletons. Recently, many exoskeletons and exosuits research groups have reported metabolic cost reduction; a Harvard research group [43] achieved a $32 \pm 9\%$ metabolic burden reduction in post-stroke walking using a tethered exosuit which is one of the notable performance among the performance of exoskeletons developed recently.

Biarticular Actuation

Despite the developments in recent years, a number of challenges need to be surmounted to achieve high metabolic cost reduction to assist people more economically. One of the remarkable challenges on designing an efficient exoskeleton is mass minimization [41, 44, 45] and more importantly, minimizing distal masses [45] has a significant effect on exoskeleton efficiency since adding any mass to the distal extremity will increase the metabolic cost of the locomotion [45] and walking pattern [44]. To address this challenge, using passive exoskeletons without any actuation and power supply module has been proposed; although the metabolic cost reduction is low, they are lightweight assistive devices [42, 46]. An alternative solution is using tethered exoskeletons in which any heavy component is grounded, and actuation is off-board [40, 47]. However, these tethered exoskeletons restrict the mobility of the exoskeleton, and experimental results have been limited to lab-based scenarios.

It has been proven that human bipedal movement is an economical locomotion [1, 48] for various terrains [1, 49] and long distances [50]. It thus inspiration for designing efficient mobile exoskeletons not only to solve the distal mass and inertia problem but also to provide some additional advantages on the exoskeleton design such as lower power consumption. One of the main reasons for human bipedal locomotion efficiency is

the presence of specific muscles, biarticular muscles [51–53], which have several unique and notable roles on human locomotion.

A human lower limb has more muscles than is needed to actuate each degree of freedom(DOF) [53] which means that human lower extremity is redundantly actuated, consisting of monoarticular muscles, which is a type of muscles spanning a joint, and another type span two joints known as biarticular muscles. Although the biarticular muscles, i.e. muscles span two joints, are not necessary for performing movements, they have not been eliminated from the human muscular system during human musculoskeletal system evolution, indicating their advantage for human locomotion [53]. Moreover, the motor control system selects certain muscles to accomplish specific tasks [54], and the metabolic energy consumption is one of the main factors to select muscles to need to be activated among the muscles of desired degrees of freedom [53]. The significance of the biarticular muscles in the energy economy of locomotion has been proven by several computational analyses [55, 56] studying biarticular muscle activation during movement.

The effect of biarticular muscles on locomotion and their benefits have been discussed in multiple studies [51, 53, 57, 58]. One of the key benefits of biarticular muscles is transporting energy from proximal to distal joints produced by monoarticular muscles [51, 59–63]; studies on jumping, which is a high power demanding task, revealed that energy produced by monoarticular muscles at each joint is not sufficient to produce a high jump [59], and energy transportation is necessary to meet the power requirement [59]. Moreover, this proximal to distal energy flow allows for the distribution of the muscles weight, resulting in lower leg inertia [63] which inherently requires less energy to be actuated, leading to more economical locomotion [53, 63]. Elftman [64] also claimed, by studying the running task, that presence of biarticular muscles can regenerate the negative work in phases of running in which adjacent joints have opposite power signs resulting in more economical movement [65] which was confirmed by [66] for walking and jumping as well.

Another central role of biarticular muscles is facilitating the coupling of joint movement [53, 57]; thereby allowing control of the distal joint. For instance, if two joints are coupled with a stiff biarticular muscle, displacement of a joint will cause the movement of another joint as well due to biarticular muscle origin movement [57]. This phenomenon is called ligamentous action [67] which permits the location of most of the monoarticular muscles away from the distal joint and indirectly control them [57]; similar to the energy transportation feature of biarticular muscles, this characteristic of biarticular muscle leads to lower inertia leg [57, 67] which can decrease the metabolic cost of locomotion.

The third remarkable benefit of biarticular muscles is controlling output force direction, which enables to get optimal output power. It has been shown that while most of the work is generated by monoarticular muscles, their output force direction is not optimal [53]. Biarticular muscles are responsible for controlling output force direction [53], which must align with velocity to reach maximum output power [53]. It has also been proven that biarticular muscles have lower contraction velocity than monoarticular muscles [57], resulting in the muscles having concurrent movements [68], and therefore higher muscle force compared to uniarticular muscles [53].

Biarticular muscle effect on limb stiffness has been studied by several researchers [69, 70]; one of the key findings is that loss of stiffness produced by biarticular muscles cannot be compensated by monoarticular muscle stiffness [69, 70]. These studies revealed that the presence of multi-joint muscles would dramatically increase the central nervous system ability to modulate endpoint stiffness [70, 71]. Additionally, biarticular muscle provides necessary coupling to regulate inter-limb interaction [72], and the absence of them would lead to elongated stiffness ellipse,

reduce maximum achievable stiffness, and finally limit orientation range [69]. The stability effect of biarticular muscles is another role that has been studied [73–75]. J. McIntyre et al. [73] proved that the presence of biarticular muscles is necessary to provide a coupling enabling passive control of neuro-musculoskeletal system stability.

Considering all these advantages and roles of biarticular muscles in human locomotion, it has inspired the robotics field researchers to adapt their designs to take advantage of biarticular biological features [53]. Several actuators [76, 77], bipedal robots [74, 75, 78], and assistive devices [53] have been designed based on multi-articular muscles configuration. The biarticular component has been used in designing several prostheses trying to mimic gastrocnemius muscle to reduce the actuators energy consumption [79–83] where results represent a promising improvement on the efficiency of prostheses [83]. Several exoskeletons and exosuits are developed also to assist two joints simultaneously [43, 47, 49, 84–86]. Asbeck et al [47] developed a soft exosuit assisting hip and ankle joints using the multi-articular concept on their design and reported 21% to 19% nominal metabolic cost reduction. Another noteworthy soft biarticular exosuit that has been designed for after stroke rehabilitation shows 32% metabolic cost reduction [43]. Quinlivan et al. [85] developed tethered multi-articular soft exosuit, which demonstrated 23% of metabolic burden reduction relative to powered of condition on healthy subject walking. Recently, Xiong et al. [87] proposed a multi-articular passive exoskeleton assisting hip and knee inspired by energy transportation feature of biarticular muscles where it stores negative mechanical work of knee joint and uses to assist hip extension, they succeeded to reduce the metabolic energy consumption by 7.6% without using any actuation module.

Simulation based Analysis of Assistive Devices

Despite all these remarkable progress that have been made on designing exoskeletons and exosuits assisting elderly and disabled subjects suffering impaired gait cycles and healthy individuals, there are remarkable challenges with experimental based studies and designing of exoskeletons. Human in the loop studies always introduce several challenges on interaction with a human, From the establishing experiments perspective, some of the challenges are providing subject-specific prototypes, recruiting appropriate volunteers, guaranteeing their safety during the experiments, and attaining ethic approvals [2]. From physical prototyping viewpoint, collecting information without implementing sensors inside the body in a limited time [2], difficulty or impossibility of some measurements [88], and training effect on subjects performance [89, 90] are some of the important challenges on human in the loop studies and designing procedures.

Simulation-based studies and designing assistive devices can complement the experimental design and analysis to overcome most of the challenges mentioned above. OpenSim is one of the software funded by NIH Roadmap grant U54 GM072970, the NIH research infrastructure grant R24 HD065690, and the DARPA Warrior Web Program and it has been used in movement science related fields [88] and it is getting so attractive for researchers in robotics, biomedical engineering, biophysics, computer science and many other fields [88, 91]. Despite all the limitations on musculoskeletal modeling and simulation [92], OpenSim enables researchers by providing biomechanical models and simulation tools to investigate the human and animals movements [88, 91]. OpenSim has been used to design and study the assistive devices [2, 93–95]. Uchida et al. [2] simulate several combinations of ideal assistive device on subjects running at 2 m/s and 5 m/s speeds and found that activity of muscles can be decreased even in the muscles that do not cross the assisted joints, and it can be increased in some muscles based on assistive device configuration; their simulation results confirmed and proposed clarification on some of the similar phenomena observed in experimental studies. Several ideal assistive devices effect on the metabolic cost of subjects carrying heavy

loads has been studied by Dembia et al. [93], their study like Uchida et al. [2] suggest the effective configurations and joints assist and give a perspective how an assistive device can change muscular activities of subjects carrying loads.

Recently, predictive simulations or simulation-based dynamic optimization approaches are emerging for studying assistive devices which can capture assistive devices effect on the musculoskeletal kinematics and kinetics [96]. This approach has been used by V. Q. Nguyen et al. [97] to study ankle exoskeleton effect on a normal speed walking subject where this approach enables them not only to study the exoskeleton effect on metabolic cost but also to investigate how the exoskeleton affects subject's kinematics and ground reaction forces. A novel active ankle powered prosthesis also was simulated and studied in predictive simulation framework by A. K. Lapre et al. [98]. Predictive simulation has also been employed to simulate knee [99] and ankle prostheses to investigate various control approaches on them [100, 101]. Moreover, Passive ankle prosthesis and Ankle-Foot orthosis stiffness has been optimized using this strategy [102, 103].

Contributions***

In this study, biarticular exoskeleton assisting hip and knee has been proposed and compared to another typical monoarticular exoskeleton. To have a methodical insight into the monoarticular and biarticular devices mechanism difference, dynamics and kinematics in motion and velocity level of each device have been derived.

Since the main objective of an exoskeleton is reducing assisted subject's energy expenditure [] and by considering all the limitations of experimental based studies discussed earlier, we implement the proposed exoskeletons mechanism in musculoskeletal simulation enabling us to not only study the devices but also analyze the musculoskeletal model of the assisted subjects.

This simulation-based study is conducted with ideal exoskeletons where devices have no mass, inertia, or any limiting factor which is beneficial to get insight into how the proposed device can affect the subjects and what is the maximum performance that we can get from the device. Additionally, since every configuration of the exoskeleton can have completely different inertial properties, using ideal exoskeletons allows us to have a fair comparison between monoarticular and proposed biarticular assistive devices.

Although studying the exoskeletons without any restriction on their performance provides handy erudition about the exoskeletons, it is necessary to analyze and compare them in more moderate performance with some constraints. This study introduced a new method to have a legitimate comparison among different configurations of the exoskeletons by taking advantage of Pareto optimization methods and implementing it in the musculoskeletal framework.

This proposed method can provide average optima points for each configuration of the assistive device based on the optimization defined objectives. In this paper, we introduced metabolic cost reduction and devices energy consumption as two optimization criteria and analyzed the devices in lower performance.

The paper is organized as follows: Dynamic Modeling section presents the kinematics and dynamics of the proposed biarticular and the monoarticular exoskeletons mechanism. Musculoskeletal Simulation then addressed the modeling of these assistive devices in OpenSim, simulations procedure, and then Pareto optimization subsection dedicated to explaining the proposed method in detail and its implementation; simulations validation procedure and the results statistical analyses explanation comes after the Pareto optimization simulations subsection. Results and their discussions are provided in the Results and Discussion section mainly separated into two main subsections, including exoskeletons results in maximum and more moderate performances; study limitation and performance metrics are also provided in

this section. Finally, this paper is concluded with Conclusions and Future Work section, which also presents future research directions.

Kinematic Modeling

The biarticular exoskeleton was designed to assist hip and knee joint. The exoskeleton has been inspired by biarticular muscles and the aim of the design was keeping the weight in proximal joint (Hip) while delivering the required power to distal joint (Knee). The parallelogram mechanism has been purposed to accomplish this goal and take advantage of biarticular muscles biological features in the exoskeleton. The purposed exoskeleton was shown in figure 1(a).

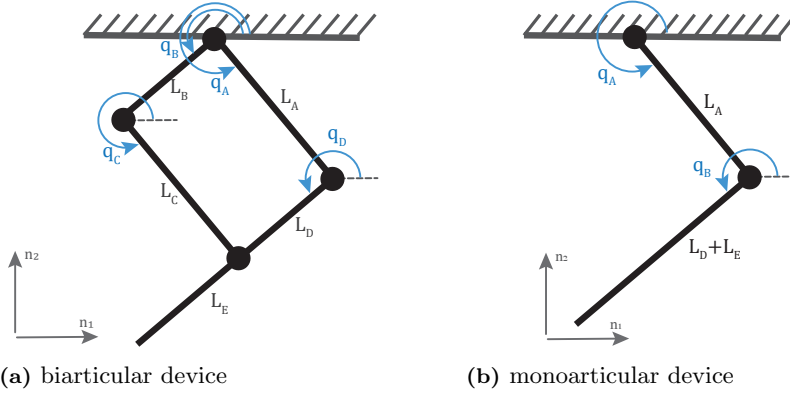


Fig 1. Assistive devices kinematics model. The parallelogram mechanism has been used to model the biarticular exoskeleton and the monoarticular exoskeleton modeled by two link serial manipulator.

Where the hip joint will be assisted by applying directly the torque on the joint and second actuator torque will be applied to knee joint through the parallelogram mechanism where kinematics is

$$x_{Bi} = l_A \cos(q_A) + (l_E + l_D) \cos(q_B) \quad (1)$$

$$y_{Bi} = l_A \sin(q_A) + (l_E + l_D) \sin(q_B) \quad (2)$$

Monoarticular Exoskeleton can be modeled as a two-link serial manipulator as shown in figure 1(b) where each joint is assisted by the directly joint actuator and the forward kinematics of monoarticular exoskeleton is:

$$x_{mono} = l_A \cos(q_A) + (l_E + l_D) \cos(q_A - q_B) \quad (3)$$

$$y_{mono} = l_A \sin(q_A) + (l_E + l_D) \sin(q_A - q_B) \quad (4)$$

For both of the exoskeletons configurations the kinematics in motion level also can be easily driven and resulted Jacobian of each configurations can be written as in Eq (5) and (6).

$$J_{Bi} = \begin{bmatrix} -l_A \sin q_A & -(l_E + l_D) \sin(q_B) \\ l_A \cos(q_A) & (l_E + l_D) \cos(q_B) \end{bmatrix}_{2 \times 2} \quad (5)$$

$$J_{Mono} = \begin{bmatrix} -l_A \sin q_A - (l_E + l_D) \sin(q_A - q_B) \\ l_A \cos q_A + (l_E + l_D) \cos(q_A - q_B) \\ (l_E + l_D) \sin(q_A - q_B) \\ -(l_E + l_D) \cos(q_A - q_B) \end{bmatrix}_{2 \times 2} \quad (6)$$

As it can be interpreted from the kinematics of exoskeletons, there is a jacobian between monoarticular and biarticular exoskeletons as it is represented in Eqn (7).

$$\omega_{2 \times 1, \text{monoarticular}} = J_{2 \times 2} \omega_{2 \times 1, \text{biarticular}}$$

$$\begin{bmatrix} \text{torso} & \omega_{\text{mono}}^{\text{femur}} \\ \text{femur} & \omega_{\text{mono}}^{\text{tibia}} \end{bmatrix} = \begin{bmatrix} 1 & 0 \\ -1 & 1 \end{bmatrix} \begin{bmatrix} \text{torso} & \omega_{\text{bi}}^{\text{femur}} \\ \text{torso} & \omega_{\text{bi}}^{\text{tibia}} \end{bmatrix} \quad (7)$$

Using Eqn.(7) which is a mapping between the angular velocities of the exoskeletons, we can derive the mapping between the provided torque by exoskeletons.

$$\tau_{2 \times 1, \text{biarticular}}^T \omega_{2 \times 1, \text{biarticular}} = \tau_{2 \times 1, \text{monoarticular}}^T \omega_{2 \times 1, \text{monoarticular}}$$

$$\tau_{2 \times 1, \text{biarticular}}^T \omega_{2 \times 1, \text{biarticular}} = \tau_{2 \times 1, \text{monoarticular}}^T J \omega_{2 \times 1, \text{monoarticular}}$$

Rewriting the equations more clearly, we can express the torque mapping explicitly as Eqn.8.

$$\tau_{2 \times 1, \text{biarticular}} = J^T \tau_{2 \times 1, \text{monoarticular}}$$

$$\begin{bmatrix} \tau^{\text{torso/femur}}_{\text{bi}} \\ \tau^{\text{torso/tibia}}_{\text{bi}} \end{bmatrix} = \begin{bmatrix} 1 & 0 \\ -1 & 1 \end{bmatrix}^T \begin{bmatrix} \tau^{\text{torso/femur}}_{\text{mono}} \\ \tau^{\text{femur/tibia}}_{\text{mono}} \end{bmatrix} \quad (8)$$

This relation between two exoskeleton has been used to verify the modeling of the exoskeleton through musculoskeletal simulation framework.

Musculoskeletal Simulation

Musculoskeletal Model

The exoskeletons have been studied through musculoskeletal simulations by conducting the simulations of the seven subjects walking normally and while carrying a 38kg load on the torso at their chosen speed. The data that has been used in this study was experimentally collected and processed by Dembia et.al. [93] and their experimental protocol was approved by the Stanford University Institutional Review Board [93].

The musculoskeletal model used in the simulations, which was the same with the model used by dembia et al. [93], was a three-dimensional model developed by Rajagopal et al. [104] with 39 degrees of freedom where the lower limbs were actuated using 80 massless musculotendon actuators, and the upper limb actuated by 17 torque actuators [104].

This three-dimensional musculoskeletal model was adapted by locking some unnecessary degrees of freedom for both normal walking and walking with a heavy load scenarios and modeling the extra load on the torso of the musculoskeletal model for the walking with heavy load condition [93].

Since this research was built upon the study performed by Dembia et al., we will follow the similar terminologies in most of the cases to avoid any confusion for the readers. Therefore, the *loaded* condition will refer to the subjects walking while carrying the 38Kg load on their torso while the *noload* condition will reference the subjects walking without any extra load at their self chosen speed.

Simulation Procedure

The first step for conducting the simulation of the specific subject is scaling the generic dynamic model to acquire a musculoskeletal model matching with the anthropometry of the subject which was performed using OpenSim Scale Tool and according to the mass and height of the subject, the maximum isometric forces of the muscles were scaled. After obtaining the specific model for the subject, inverse kinematics of the subject were computed using OpenSim Inverse Kinematics Tool and the motion capture data collected experimentally.

On the next stage of the simulation workflow, the scaled model, inverse kinematics and ground reaction forces were employed to run the RRA algorithm [91]. The RRA algorithm reduces the incompatibility of experimental data including ground reaction forces and trace data and musculoskeletal model by slightly adjusting inertial properties and kinematics. Then adjusted model and kinematics generated by RRA were employed to perform muscle driven simulations using Computed muscle control algorithm in OpenSim [105].

Computed Muscle Control (CMC) algorithm simulates the muscle recruitment of the subject by resolving muscle redundancy problem using static optimization to find the required muscle excitations to track the provided kinematics. The CMC simulations output were then used to run the analysis tool of OpenSim to compute subjects metabolic power consumption, and muscles moment.

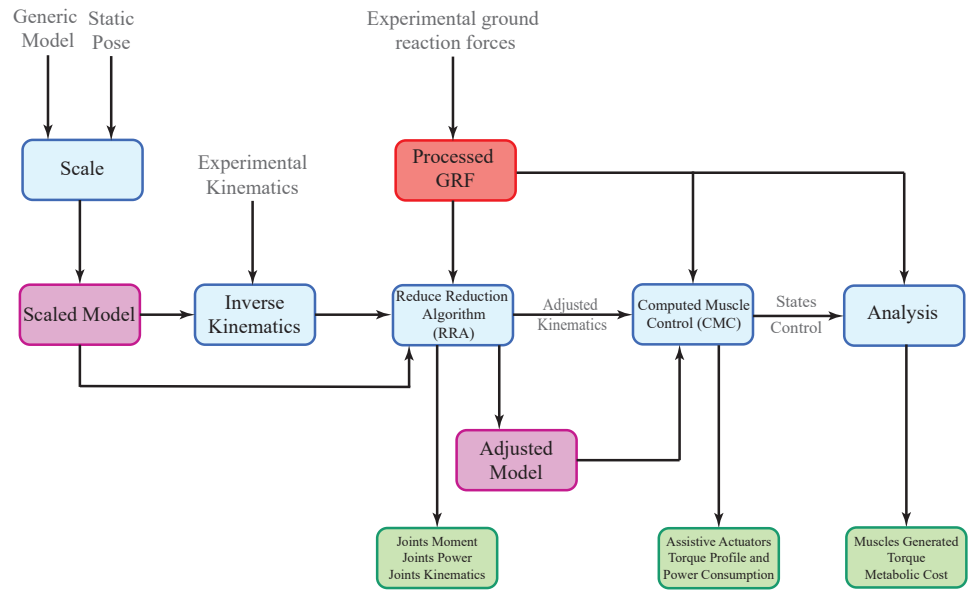


Fig 2. Opensim simulation procedure block diagram. The workflow of the simulation in OpenSim has been shown briefly in which green blocks stands for output, blue blocks are OpenSim simulations or analyses, purple blocks are models that have been used for simulations and analyses, and finally, red blocks represent processed experimental data.

The OpenSim solves the muscle redundancy problem to track experimentally measured motion and uses effort-based objective, as Eqn.(9), to solve for a set of muscle excitations to track measured motions and forces within a specified tolerance using static optimization at each time step during the motion of interest [92]. Therefore, the

kinematics and dynamics of the subject will remain consistent during the simulations and any additional mass and inertia on the subject that has not been captured by experiments will cause a systematic error on the results.

$$J = \sum_{i \in nMuscles} a_i^2 + \sum_{i \in nReserves} \left(\frac{\tau_{r,i}}{w_{r,i}} \right)^2 \quad (9)$$

With the knowledge of the OpenSim neural control algorithm, we used the adjusted model and kinematics provided by Dembia et al. [93] instead of reproducing all data from the beginning of the simulation procedure which also helped us to ease the verification of the simulations procedure thanks to [93] for verified simulations data.

Metabolic Model. To calculate the estimation of the instantaneous metabolic power of subjects, Umberger [106] muscle energetic model which was modified by Uchida et al. [107] were employed in which average power consumption of a muscle during a gait cycle was calculated using Eq.(10) [107].

$$P_{avg} = \frac{m}{t_1 - t_0} \int_{t_0}^{t_1} E(t) dt \quad (10)$$

Where m is muscle mass, and $E(t)$ is the normalized metabolic power consumed. This model generates metabolic power of all muscles and then whole body metabolic power was calculated by summing all muscles metabolic power [107]. For computing the gross metabolic energy consumption of subjects, we integrated the metabolic power over the gait cycle and then divided by the mass of subjects.

As it is mentioned in [93], due to experimental data insufficiency, some subjects and trials simulation were not a complete gait cycle, therefore, the metabolic energy were calculated for a half of a gait cycle for these subjects and trials which is a verified method for computing the energy according to [93].

Modeling and simulation of assisted subjects

The kinematics of the exoskeletons were already discussed and in order to model ideal exoskeletons in OpenSim framework we used the Torque Actuators provided by OpenSim API [91]. Biarticular and Monoarticular exoskeletons' torque actuators were assigned, as shown in figure 3. As it is represented in figure 3 (a), both torque actuators of biarticular exoskeleton were assigned to torso , then, reaction forces of the actuators were applied to the torso which is in the match with the kinematics and dynamics model of the biarticular exoskeleton.

$$\tau_{Biarticular}^{hip} = \tau^{torso/femur} \quad (11)$$

$$\tau_{Biarticular}^{knee} = \tau^{torso/tibia} \quad (12)$$

Monoarticular exoskeleton (figure 3 (b)) modeled by assigning hip joint actuator from torso to femur body and knee joint actuator assigned from femur to tibia body where knee torque actuator's reaction torque applied to femur body:

$$\tau_{Monoarticular}^{hip} = \tau^{torso/femur} \quad (13)$$

$$\tau_{Monoarticular}^{knee} = \tau^{femur/tibia} \quad (14)$$

Computed Muscle Control adjusted objective function. To investigate the performance of the assistive devices and their effect on human musculoskeletal system through OpenSim simulation framework we used the CMC algorithm. Computed

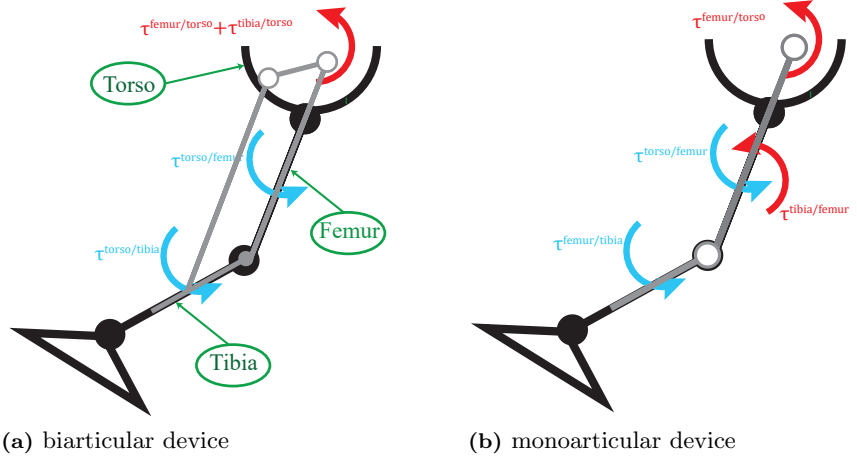


Fig 3. Assistive devices modeling on OpenSim. The modeling of the hip and knee assistive devices in OpenSim framework in which TorqueActuators provided by opensim has been utilized to model the exoskeletons. The blue and red torques represent the action and reaction torques of the assistive actuators on the bodies.

Muscle Control algorithm objective function depends on the sum of squared muscle activation and reserve actuators, which compensates for modeled passive structures and potential muscle weakness [93]:

$$J = \sum_{i \in nMuscles} a_i^2 + \sum_{i \in nReserves} \left(\frac{\tau_{r,i}}{w_{r,i}} \right)^2 \quad (15)$$

Where w_i determines the weight of reserve actuators which is generally selected as a small number to highly penalize using of reserve actuators. By adding assistive device actuators (i.e. Torque Actuators) to the musculoskeletal model of the subject they will be added to the CMC tool objective function. The adjusted objective function will include the assistive actuators as it is expressed in Eq. (16) and by selecting proper weights for the assistive actuators, they can be chosen by the optimizer as the actuation of the assigned degree of freedom.

$$J = \sum_{i \in nMuscles} a_i^2 + \sum_{i \in nExo} \left(\frac{\tau_{exo,i}}{w_{exo,i}} \right)^2 + \sum_{i \in nReserves} \left(\frac{\tau_{r,i}}{w_{r,i}} \right)^2 \quad (16)$$

In the adjusted objective function, $w_{exo,i}$ is torque actuator weights which is named optimal force in OpenSim [93] penalizing the usage of torque actuators. By selecting a large number, penalization of the actuators will be insignificant and they will be selected for actuating the joint between two bodies assigned for torque actuator and if we select a small optimal force, the optimizer will highly penalize the usage of exoskeleton actuators. To study each configuration of the exoskeleton in their maximum performance, the assigned torque actuator's optimal force was selected as 1000 N.m enabling the optimizer to use the assistive actuators as much as possible during a gait cycle simulation.

Metabolics and actuators energy calculation. Similar to the unassisted procedure, the instantaneous metabolic power of the subjects was computed using the energetic model of Uchida et al. [107] and then metabolic energy of subjects were derived by integration of the metabolic power over the gait cycle. In order to compute

the energy consumption of the assistive actuators, the power profile of the actuators were obtained and their absolute power profiles were integrated over the gait cycle and divided to the subjects mass. Similar to the energy consumption of the exoskeleton procedure, the negative energy or regeneratable energy through a gait cycle were calculated by obtaining the negative power profile and integrated over the gait cycle and normalized to the mass of the subject.

Pareto Simulations

The optimization stage of the Computed Muscle Control (CMC) algorithm uses the weighted sum of squares to solve muscles and assigned actuators redundancy to select a set of actuation with the lowest cost for tracking the kinematics of the dynamic model of the subject [92]. To investigate the ideal assistive devices maximum effect on the subjects metabolic power consumption regardless of their energy expenditure, large weights were assigned to assistive actuator.

However, in the real-time, exoskeletons are restricted by the energy that can be supplied to the actuation module and the maximum torque that the actuation module can provide to the joint of interest; to study devices performance under the maximum provable torque to the joints and their effect on musculoskeletal system in lower energy consumption regions, we used the Pareto-Optimization concept [108].

Pareto method integrates all optimization criteria in its procedure and constructs a Pareto front representing trade-off among the criteria enabling us to have optima curves for each configuration of the devices [109] and conduct a fair comparison between the exoskeletons and the load conditions. In this study, metabolic cost reduction and assistive actuators energy consumption were considered as two optimization criteria to study the trade-off between the exoskeletons and load conditions.

One of the acceptable Pareto front is a discrete set of Pareto-optima points obtained by constructing a single objective function by integrating objectives and optimizing the single cost function throughout the specific range of values of the parameters used to combine the cost functions into a single objective function [110].

The pareto optimization method has been used by M. L. Handford and M. Srinivasan [100, 101] to study robotic lower limb prostheses by simultaneously optimizing the metabolic and prosthesis cost rate.

The workflow of the Pareto-simulations. To perform the simulations of the Pareto-optimization in the OpenSim framework, we constrained the peak torque of assistive actuators constraining the objective function mentioned in Eq (16) throughout a specific range from high to low provable torque throughout a gait cycle changing the solution of the optimizer for muscles and actuator redundancy problem. This variation over the discrete range of maximum provable torque resulting in different points on the optimization objectives space and by filtering points, we achieved to Pareto front for each configuration of the exoskeleton.

For the biarticular and monoarticular exoskeletons in both *loaded* and *noload* conditions, the maximum torque of the actuators were varied between 30 N.m and 70 N.m. For performing the simulations, the constraint of the hip actuator was fixed and the constraint of the knee was varied; after simulating all of the exoskeletons with a fixed hip constraint and varying knee constraint, the constraint of the hip actuator was changed for performing the next iteration of the simulations. The algorithm has been shown the following pseudo code.

Algorithm 1 Pareto Simulations Algorithm

```
1: for  $i = [70, 60, 50, 40, 30]$  do
2:   for  $j = [70, 60, 50, 40, 30]$  do
3:     Set  $\{-i, i\}$  : hip actuators constraint:  $\{MinControl, MaxControl\}$ 
4:     Set  $\{-j, j\}$  : knee actuators constraint:  $\{MinControl, MaxControl\}$ 
5:     Update exoskeleton model by the new constraints
6:     Perform CMC Simulation
7:   end for
8: end for
```

Validation of Simulations

The comprehensive validation procedure of the OpenSim simulations was published by the Hicks et al. [92] where they explained how to validate modeling and simulation results at each stage. Additionally, Dembia et al. [93] explained simulation verification for their assistive device simulations and we followed the same procedures explained in [92, 93] to validate our results from the simulations.

As it is already discussed, the adjusted model, adjusted kinematics and processed ground reaction forces that has been provided by [93] have been used for accomplishing this study which has been evaluated and validated by Dembia et al. [93]. As it is recommended in [92], the muscular activation resulted from the simulation has been validated with the experimentally recorded electromyography (EMG) signals.

The *loaded* and *noload* joint kinematics and kinetics were compared with the results of the studies accomplished by Huang and Kuo [111] and Silder et al. [112] and validated qualitatively. Since our simulations of the unassisted subject for *loaded* and *noload* conditions were the same with Dembia et al. simulations, we reproduced their simulations and compared them with their results to validate our reproduced simulations results. Additionally, since we used the provided RRA results for performing the CMC simulations, the joint moment and joint kinematics represented in this paper were already validated.

The other source of error during the simulations are kinematics and residual errors which were analyzed to be in the recommended thresholds [92]; nevertheless, since the inverse kinematics stage of simulation was not reproduced in this study, the markers error was not examined. Another error source in these simulations could be additional moments introduced to compensate any modeled passive structures and muscles weakness where it is recommended to have less than 5% of net joint moments in peak and RMS [92]. It has been checked for all simulations and confirmed that the reserve actuator torques are smaller than the recommended percentage of joint moments.

Performance Metrics

For the purpose of having methodical analysis and comparison between the assistive devices and load conditions some performance metrics have been defined. As discussed earlier, the ultimate goal of each assistive device is reducing energy consumed by the subject for performing a task which is walking with and without load at normal speed in this study. Therefore, we calculated the normalized gross whole-body metabolic rate of the subjects in two different assistive devices and load conditions and then metabolic cost reduction has been computed using the metabolic rate of assisted and unassisted subjects. This procedure of metabolic cost calculation was repeated for all seven subjects in three trials to obtain the total average metabolic energy expenditure and metabolic cost reduction for each assistance scenario and load condition.

Another important metrics for assessing the performance of an exoskeleton is the

energy it consumes to provide the assistance. To analyze this metrics in the simulated exoskeletons, we computed the absolute energy consumed by the all actuators and the reason for considering the absolute value is absence of the regeneration mechanism as a general case for the exoskeletons. On the other hand, in order to analyze the amount of energy available for regeneration, we computed the negative energy of the exoskeletons. This metric is a crucial part of the untethered exoskeletons analysis to estimate the battery life.

At the pareto optimization part of the study, these two metrics (i.e., metabolic cost reduction and energy consumption) are represented together by averaging them for each defined constraints over the subjects and represented with mean and standard deviation for both criteria. This metric represents the set of different configurations for each exoskeleton in terms of energy consumption and the amount of assist the device can provide. For more detailed analyses, some specific configurations in each exoskeleton and load condition have been selected and compared in more comprehensive manner.

Additionally, the effect of regeneratable energy and inertial properties of the exoskeletons, as two important metrics for analyzing the performance of the assistive devices, have been studied in pareto simulations by reflecting their effect on the Pareto-curves and obtaining the pareto sets affected by these two metrics. Finally, some of the muscular activations of the lower limb key muscles were extracted and studied to have insight into how an assistive device can change muscles activities and consequently, metabolic cost which is resulted from muscles activities.

Statistical Analysis

To conduct methodical comparisons among scenarios with the discussed metrics, we employed statistical analyses. Since the simulations were performed on seven subjects with three trials in five different scenarios, repeated measures analysis of variance (ANOVA) and Tukey Post-hoc were applied to test the statistically significant difference between the selected metrics and scenarios. Additionally, for the pareto simulations, the statistical analysis has been performed for the specific points selected from the pareto front for further investigation, nevertheless, standard deviation of all points on pareto front has been explicitly plotted for both criteria. We used a significance level of 0.05 and SPSS [113] for performing the tests. Same as [93], to remove the hierarchical structure from the data, they were averaged over the trials for each subject-scenario pair. However, the time-dependent data are averaged over all subjects and their trials and represented by their mean and standard deviation.

Results and Discussion

Ideal Exoskeletons Results

Device Performance

Both biarticular and monoarticular configurations of the ideal exoskeletons reduced the metabolic energy consumption of subjects walking without and with carrying a heavy load at self-selected speed walking. Biarticular and monoarticular exoskeletons decreased the subjects carrying a heavy load metabolic rate by $20.49 \pm 2.87\%$ and $20.45 \pm 2.81\%$. The monoarticular and biarticular configurations of the exoskeleton were able to reduce the gross whole-body metabolic cost of the subject in the *noload* condition by $22.38 \pm 4.91\%$ and $22.47 \pm 4.89\%$. These exoskeletons were expected to have the same performance on reducing the metabolic energy consumption of the subjects due to their kinematic relation, and the results are representing the expected performance for these two devices.

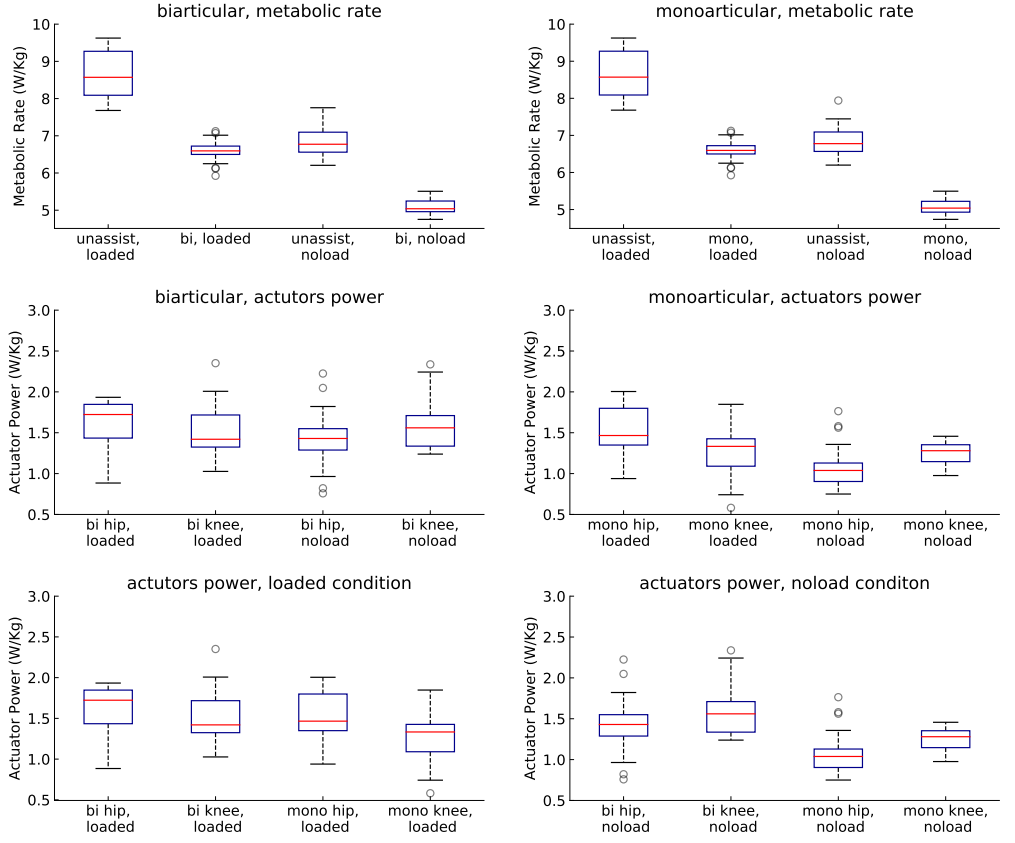


Fig 4. Assistive devices and metabolic power. The power consumptions of assistive devices and their effect on whole-body metabolic rate of the subjects walking with and without carrying a heavy load.

The assistance of both exoskeletons on subjects carrying a heavy load was able to compensate for demanding metabolic energy for carrying the heavy load. As it can be seen in figure 4, the assisted subjects in *loaded* condition have a similar metabolic rate with unassisted subjects do not carry any load meaning that the best both ideal exoskeletons can do is reducing the metabolic energy-demanding of the *loaded* subject to subject without any load.

The energy consumption of both exoskeletons has a high within-subject variation on the *loaded* condition comparing to the *noload* condition. While monoarticular exoskeleton had less energy consumption in both knee and hip actuators and both conditions, but these differences are not statistically significant between the two exoskeletons. Although both exoskeletons have considerably different hip actuator energy consumption between *noload* and *loaded* conditions, the significant difference between the loading conditions of the subjects cannot be observed for energy expenditure of the knee actuator in both configurations.

Devices Speed, Torque and Power

One of the main objectives of this section is to validate the kinematic modeling of the exoskeleton on OpenSim. As it is already discussed, there is a mapping between monoarticular and biarticular exoskeletons, and if the modeling of the devices were

correct in the musculoskeletal simulator, this kinematics relation requires to be held.

The figure 5 represents the velocity profiles of the biarticular and monoarticular exoskeletons in both load conditions. From the Eqn. (7) we were expecting to have the same angular velocity profiles hip actuator, and since hip actuator in both exoskeletons were supposed to be attached directly to the hip joint, the velocity of the joint and actuators in both devices have practically the same profiles as it is shown in figure 5 for hip joints in both load conditions.

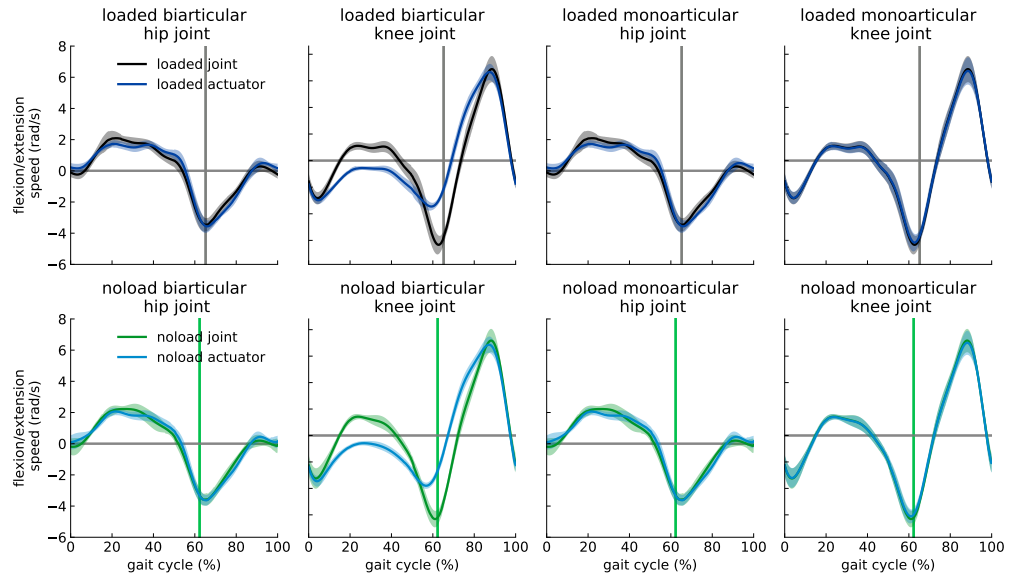


Fig 5. Assistive devices velocity profiles compared to joint required velocities.

The device actuator velocity for subjects carrying heavy load (dark blue) and without any load (blue), and net joint velocity profile for *loaded* (black) and *noload* (green) conditions are shown for each actuator of the devices. The curves are averaged over 7 subjects with 3 trials; shaded regions around the mean profile indicate standard deviation of the profile.

The main difference between the two configurations of the exoskeleton is on the knee joint, where the biarticular device assists the joint through a parallelogram mechanism, and the velocity profiles of the knee actuator were supposed to be different according to their jacobian. This difference can be seen in the figure 5 where monoarticular knee actuator follows the knee joint velocity profile, but the biarticular actuator is showing different profile than the knee joint profile due to Eqn. (7). Analyzing velocity profiles of the devices validating the mapping between two exoskeletons and modeling of them through OpenSim.

According to the jacobian between these two devices expressed in Eqn. 8, the knee and hip actuators were expected to have the same and different torque profiles respectively, which is evident in figure 6 for both *loaded* and *noload* conditions. The generated optimal torque profiles of the ideal exoskeletons did not resemble the net moment of the assisted joint, which was also observed by [2, 93] for the simulation-based study of the walking with heavy load and running respectively. The torque of assistive actuators in both hip and knee joints exceeded the corresponding net joint moment and resulted in opposing muscles generated moment and device torque in the joint.

This antagonism is more significant on the knee joint than hip during the mid-stance phase to the mid-swing phase, with the highest opposition on the start of the pre-swing phase. The hip joint has significant actuator and muscle torque opposition during the

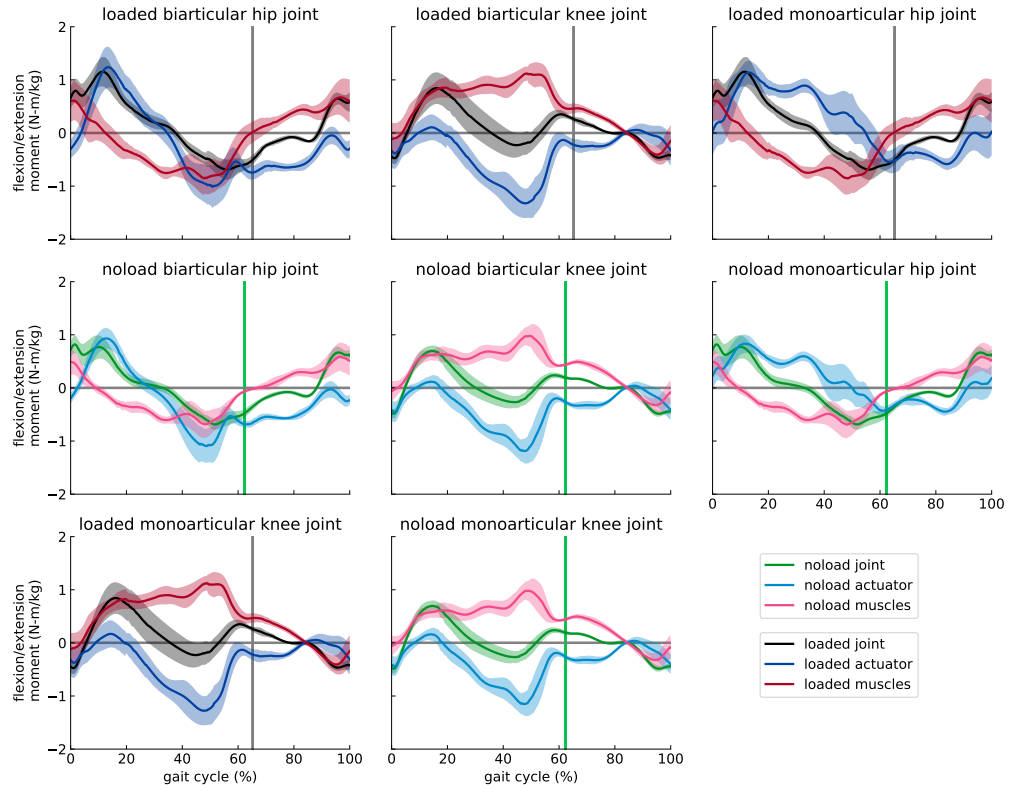


Fig 6. Assistive devices torque profiles compared to joint and muscles generated moment. The device actuator torque for subjects carrying heavy load (dark blue) and without any load (blue), net joint moment profile generated by unassisted muscles for *loaded* (black) and *noload* (green) conditions, and the generated moment by assisted muscles for *loaded* (dark rose red) and *noload* (rose red) conditions are shown for each actuator of the devices. The curves are averaged over 7 subjects with 3 trials and normalized by subject mass; shaded regions around the mean profile indicate standard deviation of the profile.

pre-swing to terminal swing phases meaning unlike the knee joint in which major portion of antagonism happens during the stance phase; the hip is getting into muscle and actuator torque contraction during swing phase.

The torque profiles represented in figure 6 indicate that the loading subject with a heavy load does not result in substantial changes in the torque profiles of the assistive devices. The main changes between *loaded* and *noload* conditions are the timing and magnitude of the profiles, which is due to the change of the joints kinematics and kinetics. Nevertheless, the standard deviation of assistive devices and assisted muscles generated torques are considerably greater in the *loaded* condition, and it is more evident in the knee joint where the net joint moment has a remarkable deviation during the stance phase. This high within-subject deviation of torque profiles indicates that the assistance of subjects carrying heavy load requires the subject-specific design of the exoskeletons [2].

Due to the discussed kinematic differences between two configurations, the power profile of the exoskeletons were different in both actuators as it is represented in figure 7. The magnitude of mechanical work performed by the biarticular actuators are higher than monoarticular mechanical work, and their profiles are different during the gait

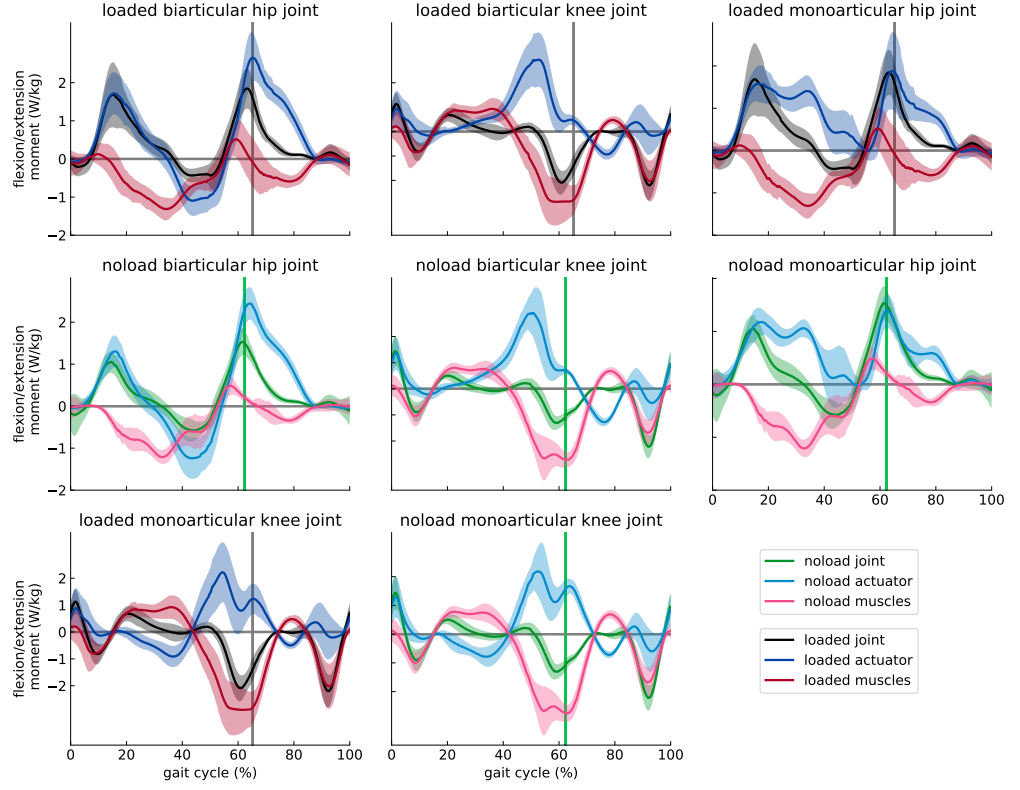


Fig 7. Assistive devices power profiles compared to joint powers. The device actuator power for subjects carrying heavy load (dark blue) and without any load (blue), and net joint power profile for *loaded* (black) and *noload* (green) conditions are shown for each actuator of the devices. The curves are averaged over 7 subjects with 3 trials and normalized by subject mass; shaded regions around the mean profile indicate standard deviation of the profile.

cycle except in the loading response and partially in mid-stance phases. The load carried by subjects causing different timing and magnitude than subjects walking with no load and the deviation of the profiles are higher for the *loaded* subject, which both are observed in torque profiles as well.

Although the power profiles of hip actuators were roughly following the net joint power profile, the knee actuator profiles not resembled the knee joint power. The mechanical work performed by the assistive devices were mostly positive work for both knee and hip actuators. The negative mechanical work in the biarticular exoskeleton can be harvested mostly during the initial-swing and mid-swing phases for the knee actuator and terminal phase for the hip actuator. Unlike the biarticular device, the monoarticular hip actuator performed practically no negative mechanical work, and the regeneratable work of the knee actuator is within both mid-stance and late-swing phases.

Device Effect on Subjects Muscles

The muscular activation of the subjects assisted by ideal assistive devices has been considerably altered. Appending a set of ideal actuators with high optimal force (i.e., low penalization) to the musculoskeletal model changes the solution of the optimizer for finding a set of actuators to track the kinetics and kinematics of the joints.

The effect of appending ideal actuators not necessarily decreases the activity of all

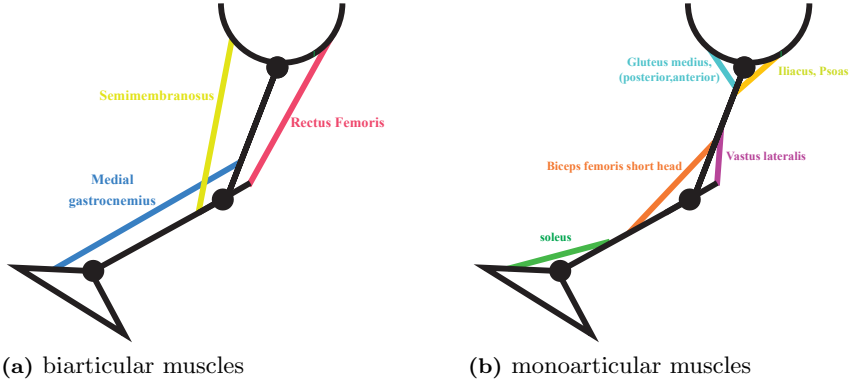


Fig 8. Biarticular and monoarticular representative lower extremity muscles

muscles, and it can be more economical for the complete set of actuators to increase the activity of specific muscles during some phases of gait to decrease the activity of less cost-effective muscles. Since metabolic power of muscles is a function of their activity, and their fiber properties [107], the reduction in the activity of the entire set of muscles is resulting in gross whole-body metabolic cost reduction.

Despite the kinematic difference between the two configurations of the assistive device, the applied torques to the joints are practically identical, and it resulted in an identical effect on the muscular activation of the subjects.

The reason for this issue rooted in the ideal nature of the actuators and devices, meaning that there are no constraints on the torque actuators can provide, the devices are assumed to be massless, and actuators do not have any reflected inertia effect. The muscle activation in figure 9, which is showing the effect of the biarticular device on the activation of representative muscles, is sufficient and can be generalized for both configurations of the assistive device.

The devices affected the activity of muscles throughout the lower extremity. This effect was significant on the Bicep femoris short head, Semimembranosus, and vasti muscles, where their activation has been replaced by another set of actuators, including muscles and ideal actuators. The rectus femoris, which is a large knee extensor and hip flexor biarticular muscle, activity has been considerably increased during the stance phase. This occurred so that the optimizer could take advantage of the rectus femoris high force-generating capacity to exert hip flexion and knee extension moments more economically. In the meanwhile, this high muscular activity of the rectus femoris resulted in high knee extension and hip flexion moments exceeding net joint moment of the joints that have been neutralized by ideal actuators, which are extremely economical for applying high torques due to its high optimal force assignments.

This set of activation in which hip flexion and knee extension required moment could be applied by more cost-effective muscles and actuators resulted in a substantial reduction in the activity of psoas and iliacus muscles as two major hip flexor muscles and the vasti muscles (vastus lateralis, vastus intermedius, and vastus medialis) as knee extensor set of muscles. The semimembranous muscle is another biarticular muscle contributing to hip extension and knee flexion moments, which has been affected by the assistive devices, and the new set of actuation has practically replaced its activity. The medial gastrocnemius as a critical knee flexor and ankle plantar flexor muscle has been affected by the assistive devices in which its activity has been substantially reduced, yet the muscle remained partially active to supply an ankle plantarflexion moment. The reduction of ankle plantarflexion moment has been compensated by increasing the

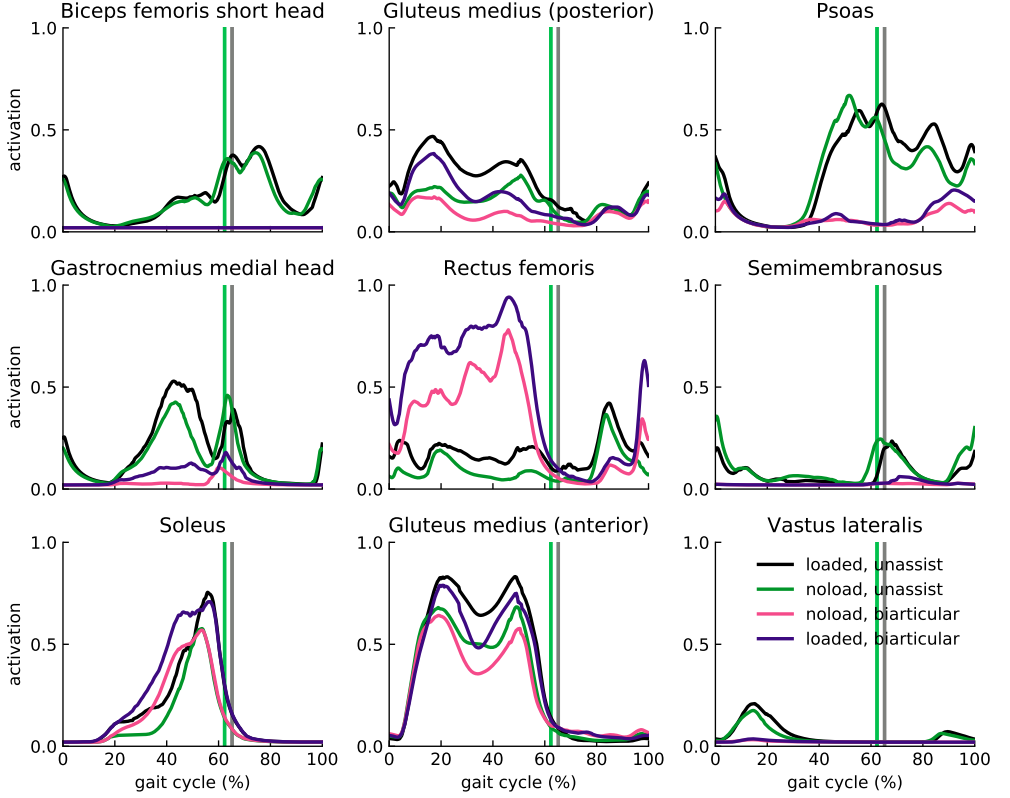


Fig 9. Activation of representative lower limb muscles of assisted and unassisted subjects. The activation of unassisted subjects carrying heavy load (black) and without any load (green), and assisted subjects in *loaded* (dark violet) and *noload* (pink) conditions are shown for nine important muscles. The curves are averaged over 7 subjects with 3 trials.

activity of soleus as another primary ankle plantarflexor muscle. The assistive devices affected the activity of the gluteus medius muscles as well, which are not only responsible for a large fraction of hip abduction moment, but also they contribute to hip motion in the sagittal plane as well and hip rotation.

The anterior and posterior portions of the gluteus medius muscle, besides their primary contribution to hip abduction, were supporting the hip extension and flexion and its lateral and medial rotations. However, the contribution of these muscles to the hip sagittal moment replaced by assistive devices and a modified set of activations in assisted subjects, and it resulted in their muscular activity reduction.

The main differences between the muscular activity of the subjects walking normally and subjects walking while carrying a heavy load on torso are the magnitude and timing of the muscular activations which were observed already in other profiles as well. This load condition affected partially some muscles like Semimembranosus in which the device did not completely replace by the ideal devices.

Pareto Simulation Results

The assistive devices analyzed in the previous section, and their effect on metabolic cost and muscular activation of the subjects in two different load conditions have been studied. The simulations of the previous section were performed under the assumption

that the assistive actuators have no bounds on the amount of the moment they can supply to the musculoskeletal model. However, this assumption is not a descriptive assumption for the real-time designing and controlling assistive device because the devices and especially untethered exoskeletons have some constraints on the amount of moment that their actuation unit can provide to assist the joint of interest and the suppliable energy from the battery for untethered exoskeletons is limited by the battery life.

One of the main aims of Pareto simulations was addressing this limitation through a simulation-based study in which we can analyze the performance of assistive devices under the limitation of their actuators on providing torque to the joints. The study has been accomplished by constraining the peak torque the assistive actuators can provide, and the optimal trade-off between the metabolic cost reduction and energy consumption of the devices has been obtained. The average Pareto front for the biarticular and monoarticular exoskeletons for both loading conditions of the subjects are represented in figure 10.

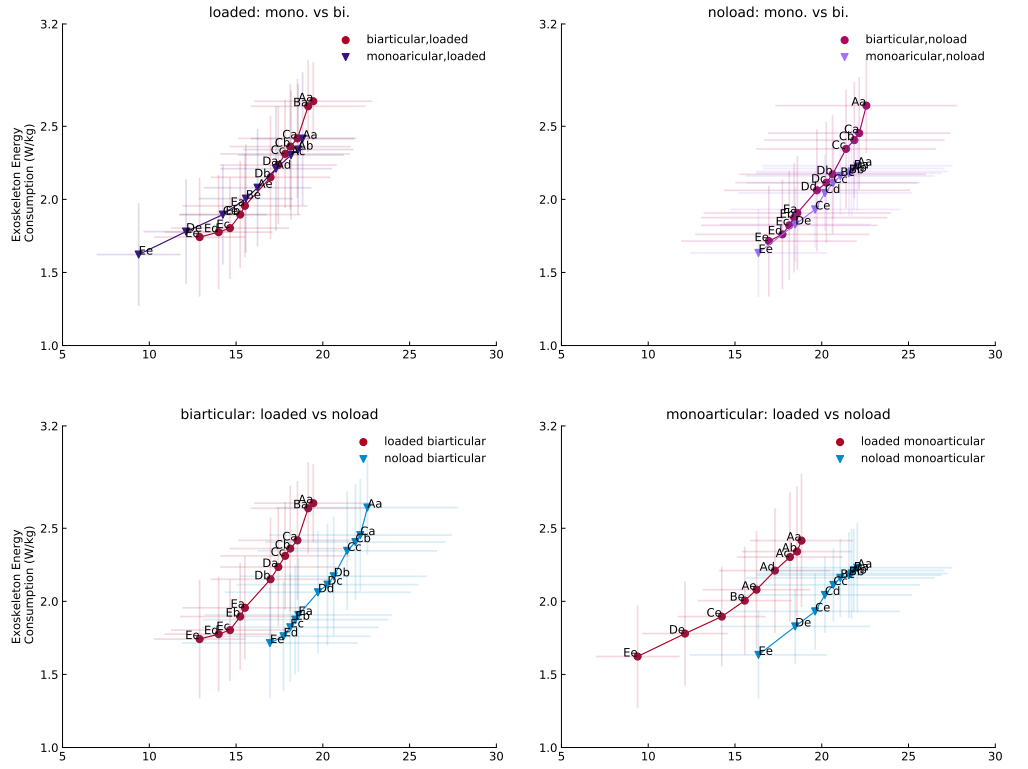


Fig 10. Optimal trade-offs between metabolic cost reduction and device energy consumption. The label on each marker is denoted to results from different peak torque constraints. The hip and knee constraints are labeled from A to E and a to e respectively. The A, a to E, e labels represent for 70 N.m to 30 N.m constraints respectively, and each marker, which stands for a specific configuration of a device, is labeled by the hip and knee constraints labels. The optima points on Paretofronts are resulted from averaging over 7 subjects.

One of the immediate implications these Pareto fronts are providing is that the constrained devices in their maximum torque bounds where hip and knee restricted to 70 N.m peak torque, can mostly provide assistance that has been provided by the ideal exoskeletons with lower energy consumption in both load conditions (Table 1). Both

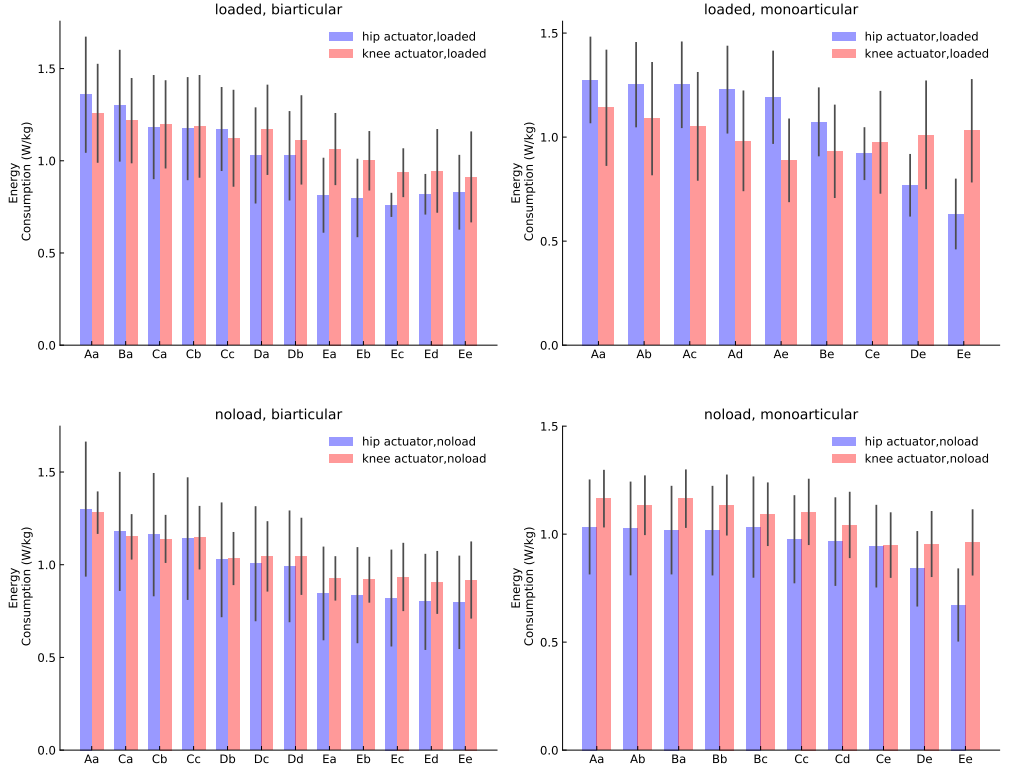


Fig 11. Energy consumption of optimal assistive actuators. The horizontal axis shows the device number on the optimal pareto-front. The vertical lines represent the standard deviation of devices in 7 subjects.

constrained devices were able to assist the *noload* subjects as much as the ideal exoskeletons were assisting, whereas the energy consumption in the biarticular exoskeleton was reduced considerably compared to its ideal actuation, but the monoarticular energy consumption was practically the same with its ideal configuration.

Similar to the *noload* condition, the constrained devices had a high metabolic reduction in the *loaded* subjects; even though it was not the same with the ideal configuration of the devices, the energy consumption had a considerable reduction, especially in the biarticular configuration which is the same as the *noload* condition. The performance of devices under peak torque limitation and its comparison with the ideal devices implies that the comparison of assistive devices with unlimited actuation units is not a legitimate comparison suggesting that the comparison between assistive devices should be conducted using optimal trade-off points of devices in which a device has its optimal performance in both energy consumption and metabolic cost reduction criteria.

The biarticular and monoarticular exoskeletons are showing practically similar performance in assisting subjects with and without load. Nevertheless, analyzing the energy consumption of the devices on the Pareto front reveal that the monoarticular device considerably affected by the load condition of subjects in which the performance of monoarticular exoskeleton became practically identical with the biarticular device when subjects were *loaded* whereas the monoarticular device had superior performance in *noload* condition.

The detailed analysis of the monoarticular device show that both actuators of this

Table 1. Device performance in with ideal and constrained actuators.

configuration	device type	condition	hip energy consumption (W/kg)	knee energy consumption (W/kg)	metabolic cost reduction (%)
biarticular	ideal	<i>noload</i>	1.42 ± 0.32	1.58 ± 0.30	22.38 ± 4.91
	ideal	<i>loaded</i>	1.58 ± 0.29	1.52 ± 0.29	20.49 ± 2.87
	constrained	<i>noload</i>	1.30 ± 0.36	1.28 ± 0.29	22.57 ± 4.92
	constrained	<i>loaded</i>	1.38 ± 0.36	1.27 ± 0.29	19.54 ± 2.79
Monoarticular	ideal	<i>noload</i>	1.09 ± 0.24	1.24 ± 0.13	22.47 ± 4.89
	ideal	<i>loaded</i>	1.52 ± 0.28	1.24 ± 0.27	20.45 ± 2.81
	constrained	<i>noload</i>	1.06 ± 0.22	1.16 ± 0.12	22.05 ± 5.18
	constrained	<i>loaded</i>	1.27 ± 0.19	1.10 ± 0.26	18.68 ± 2.36

device were affected by loading subjects with a heavy load (figure 10 and 11), and unlike the *noload* condition where knee actuator energy consumption was dominant to the hip in all optimal devices, loading subjects increased the amount of mechanical work performed by the hip. In contrast, the energy consumption of the biarticular knee and hip actuators was not affected noticeably by loading subjects as figure 11 representing the energy consumption of optimal devices. Additionally, the optimal configurations of the biarticular exoskeleton are mostly similar in the subjects walking while carrying a heavy load and walking normally, whereas monoarticular exoskeleton has different configurations in both load conditions. The practically similar configurations and the performance of the biarticular exoskeleton in both load conditions can facilitate designing a biarticular device and developing a generic controller to assist the subjects in different load conditions.

Optimal device torque and power profiles

The torque profiles of constrained optimal devices slightly differed from the net joint moment of the hip, and the knee joints and the general torque trajectories of these actuators were mostly similar to the torque profiles of the devices with ideal actuators. The ideal and constrained torque profiles of biarticular hip actuators had mostly magnitude differences during mid-stance and terminal-stance to terminal-swing phases. In contrast to the hip actuator, the knee actuator has practically the same profile with the ideal knee actuator during the swing phase, but the path and magnitude of the knee actuator were mostly different from the ideal device. This comparison between the ideal and constrained devices is mostly valid when subjects were walking without carrying any load, and the only difference was the magnitude of the constrained profiles.

Both actuators of the constrained monoarticular device have different profiles with the ideal device. The hip actuators had a significant magnitude difference during the load response phase, and most of the optimal constrained hip actuators were saturated during mid-stance and terminal stance phases, which was affecting the trajectory as well. The difference between hip actuators became highly significant during pre-swing to mid-swing phases, where the torque trajectories of the constrained hip actuator were not only different from the ideal actuator but also there was high variation among optimal constrained actuators. The monoarticular knee had more resemblance to the ideal knee actuator torque profile where they had practically identical profiles during the swing phase, and the difference between them was the higher torque magnitude during the mid-stance and lower magnitude during the pre-swing phases.

Unlike the biarticular exoskeleton, where the load condition had only effect on the

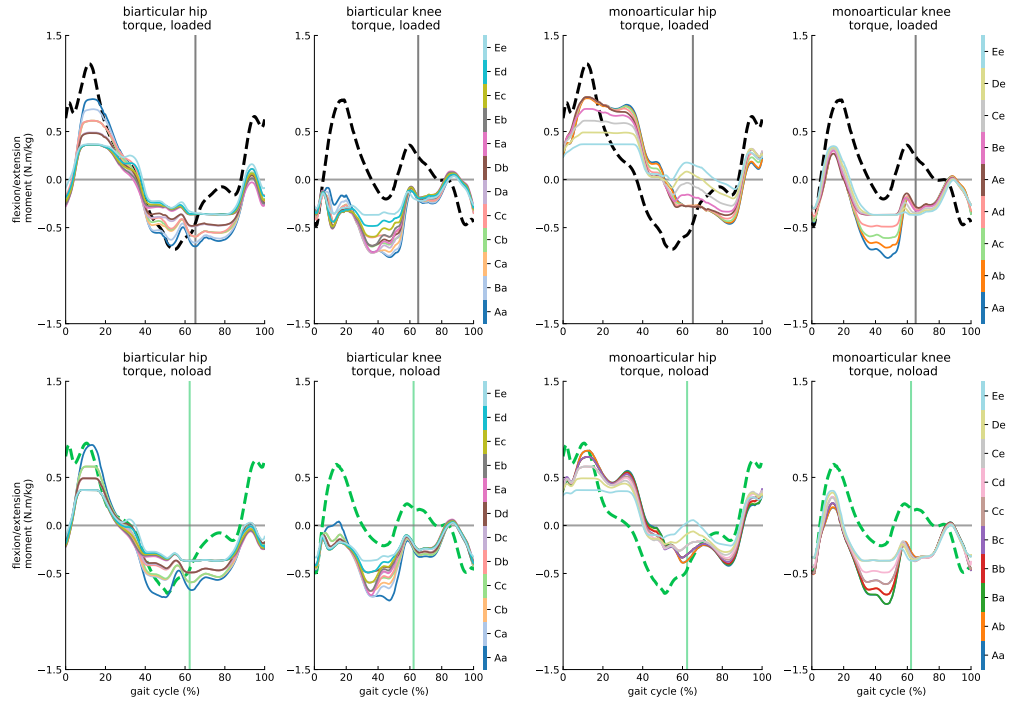


Fig 12. Optimal assistive devices torque profiles compared to joint moments.

Each line represents the torque profile of a different optimal device defined in the color bar. The label on each marker is denoted to results from different peak torque constraints. The hip and knee constraints are labeled from *A* to *E* and *a* to *e* respectively. The *A*, *a* to *E*, *e* labels represent for 70 N.m to 30 N.m constraints respectively, and each marker, which stands for a specific configuration of a device, is labeled by the hip and knee constraints labels. The profiles are averaged over 7 subjects with 3 trials normalized by subject mass.

magnitude of the profiles, and there was a close similarity between the torque trajectories in *loaded* and *noload* conditions, the hip actuator torque of the monoarticular device assisting the subjects walking without carrying any load had considerable differences with the *loaded* condition device. These two profiles had two mostly different trajectories and magnitudes during all phases of a gait cycle, and their differences are more unambiguous during load response to mid-swing phases.

The restrained biarticular and monoarticular devices had a resemblance to the ideal devices similar to the torque profiles similarity to ideal profiles. The biarticular hip actuator has mostly a similar power trajectory for the hip in both load conditions with considerably lower magnitude for all optimal devices where this magnitude difference is more substantial during mid-stance and initial swing to mid-swing phases; while the knee actuator has a high correlation with the ideal actuator, the loading response and mid-stance phases of the constrained knee actuator is different with the ideal actuator like the torque profile. The constrained monoarticular hip actuator has a high variation within optimal devices, and most of the optimal configurations have their unique power profile; nevertheless, the optimal devices with the highest peak torque limitations have a close resemblance to the ideal device. In contrast to the hip actuators, the power trajectories of the knee actuator in both load conditions were similar to the ideal device with a difference during pre-swing to mid-swing phases where the peak power consumption occurs about the toe-off in the constrained knee actuators.

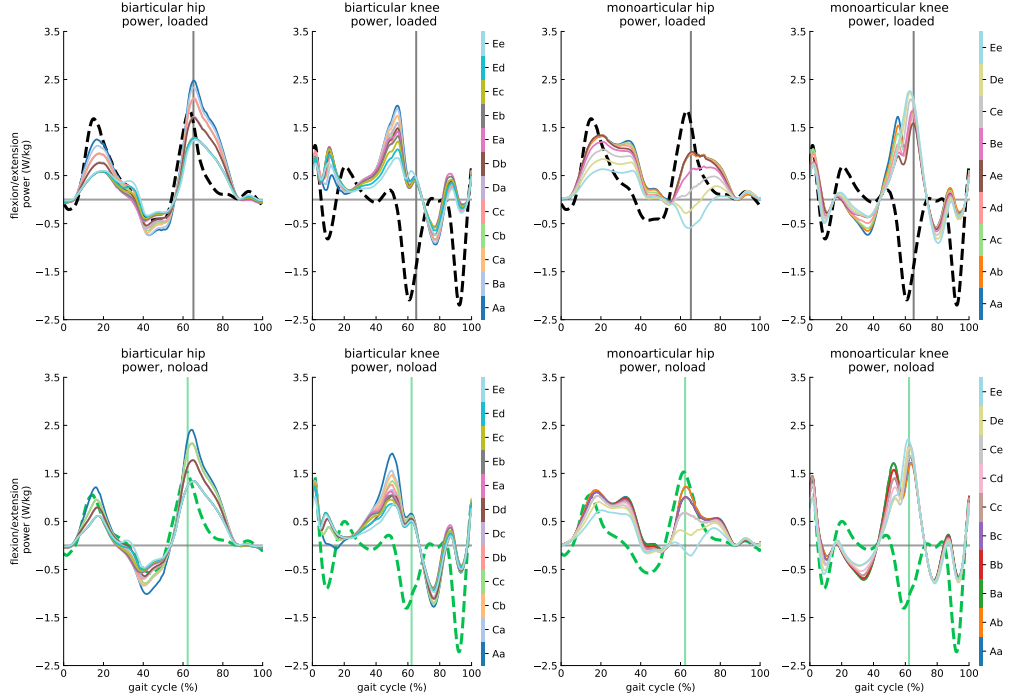


Fig 13. Optimal assistive devices power profiles compared to joint power. Each line represents the power profile of a different optimal device defined in the color bar. The label on each marker is denoted to results from different peak torque constraints. The hip and knee constraints are labeled from *A* to *E* and *a* to *e* respectively. The *A*, *a* to *E*, *e* labels represent for 70 N.m to 30 N.m constraints respectively, and each marker, which stands for a specific configuration of a device, is labeled by the hip and knee constraints labels. The profiles are averaged over 7 subjects with 3 trials normalized by subject mass.

The power and torque profiles of optimal biarticular and monoarticular devices revealing that although the optimal monoarticular exoskeletons have a lower energy consumption comparing to the optimal biarticular devices, the variation of the torque and power profiles within optimal configurations of the monoarticular device is higher than biarticular devices and load condition of the subjects can considerably affect the profiles of assistive actuators. These variations within optimal monoarticular devices indicate that achieving a generalized design and control policies for assisting subjects in different load conditions and different actuation and battery life limitations would be genuinely challenging with monoarticular exoskeletons.

Mass, inertia and regeneration effects

Inertial properties of the exoskeletons effect on metabolic rate. One of the main challenges with designing the mobile exoskeletons is the effect of the mass and inertia, grounded on the extremities of the subjects, on the metabolic rate of the subjects. The effect of mass and inertia on the metabolic cost has been studied through several literatures [114, 115] and it is shown that the metabolic rate of the subject would change considerably by adding mass and inertia [114–116].

The proposed exoskeletons in this study have a remarkably different inertial properties due to their kinematic design that will result in different effect on the metabolic energy consumption of the subjects. Since the current neural control

algorithm of the OpenSim is not able to simulate any variations in the musculoskeletal model [92], which has not been captured by experimental data, we simulated the effect of the mass and inertia offline using the model proposed by Browning et al. [114] for the effect of the mass and inertia on the metabolic cost of subjects.

The study, accomplished by Browning et al. [114], proposed a linear model for the effect of adding mass and inertia on each segment of lower limbs by capturing and analyzing the effect of adding mass to different segments of lower extremity and their inertia on the metabolic energy expenditure of the subjects experimentally. In this study, subjects were walking at 1.25 m/s without carrying any heavy load on their torso which is similar to the data captured from the subjects in the walking with *noload* at their self-selected speed [93]. This qualitative match between the data and experimental protocols of Browning et al. and Dembia et al enabling us to use the developed model of [114] to study the effect of mass and inertia added by assistive devices through offline simulations for the subjects walking at free speed without carrying any external load (i.e. *noload* condition).

The mass and inertia of the proposed biarticular and monoarticular exoskeletons affect the waist, thigh and shank segments. As it is discussed in the Kinematic Modeling section, the biarticular exoskeleton, unlike monoarticular one, is designed to deliver the assistance distally to the knee joint. It enables designers to attach actuation module to the waist instead of thigh meaning that the main difference between inertial properties of two exoskeletons will be on the attached mass on the waist and shank segments nevertheless the reflected inertia of the actuation module will be reflect on the actuated joint regardless of its grounded segment in both exoskeletons.

For the purpose of conducting numerical simulations of the inertial properties of the exoskeletons effect on the subjects metabolic rate, we assigned two identical masses and the center of masses measured from the hip ?? joint for the links attached to the thigh and shank. Additionally, a typical and identical actuation module inertia and mass has been assigned for both configurations of the exoskeleton.

In order to study the effect of the inertia in the pareto simulations, the maximum achievable torque of the actuator has been set to 2 N.m which can be provided by MaxonMotor EC90 Flat 260W and the required transmission ratio is calculated by diving the peak torque at joint level to peak torque of the actuator and then reflected inertia has been calculated using Eqn.(17).

$$R = \frac{\tau_{max,jointlevel}}{\tau_{max,actuator}} \quad (17)$$

$$I_{reflected} = I_{actuator} \times R^2$$

The total inertia of the moving segments (i.e., thigh and shank segments) have been computed by considering the distal mass effect on the inertia, reflected inertia of the actuation module and the leg inertia provided by [114] which is calculated about the hip joint in the body frame. The Eqn.(18) represents the inertia calculation of the moving segment.

$$I_{Exo,segment} = I_{reflected} + m \times COM^2 \quad (18)$$

$$I_{loaded\ leg} = I_{Exo,segment} + I_{noload\ leg}$$

The typical mass, the center of mass, and inertia that have been used for numerical simulations are represented in Table 2. The mass of each segment is within range of exoskeletons' weight studied by Mooney et al. [41] for calculating the augmentation factor and the center of mass of the segments were mostly chosen based on the mean length of thigh and shank segments [117] under the assumption of unity distribution of link weight.

The metabolic model proposed by Browning et al. [114] calculates the metabolic rate of the subject with loaded segment; however, Since we were interested in the effect of

Table 2. Mass and inertia properties of two typical exoskeletons.

configuration	Waist	thigh		shank		actuator
	Mass (kg)	mass (kg)	COM (m)	mass (kg)	COM (m)	inertia ($kg.m^2$)
Biarticular	4.5	1	0.23	0.9	$0.18 + l_{thigh}$	5.06×10^{-4}
Monoarticular	3	2.5	0.30	0.9	$0.18 + l_{thigh}$	5.06×10^{-4}

inertial properties of exoskeleton on metabolic rate change, not metabolic rate, we used the model by subtracting the metabolic rate of the subject walking without the additional mass. The equations of the final model that has been used for analyzing the effect of exoskeleton mass and inertia on the metabolic rate is provided in Eqn.(19) and (20) respectively.

$$\begin{aligned}\Delta MC_{Waist} &= 0.045 \times m_{Waist} \\ \Delta MC_{Thigh} &= 0.075 \times m_{Thigh} \\ \Delta MC_{Shank} &= 0.076 \times m_{Shank}\end{aligned}\quad (19)$$

$$I_{ratio} = \frac{I_{Exo,segment} + I_{unloaded\ leg}}{I_{unloaded\ leg}}$$

$$\begin{aligned}\Delta MC_{Thigh} &= ((-0.74 + (1.81 \times I_{Thigh,ratio})) \times MC_{unassisted}) - MC_{unassisted} \\ \Delta MC_{Shank} &= ((0.63749 + (0.40916 \times I_{Shank,ratio})) \times MC_{unassisted}) - MC_{unassisted}\end{aligned}\quad (20)$$

The effect of the exoskeleton mass and inertia has on metabolic cost has been considered on the pareto curves and filtered to obtain the pareto front with the effect of the exoskeleton inertial properties on metabolic expenditure.

Regeneration effect on devices power consumption. The significant energy requirement of the untethered exoskeletons and the finite energy density of the power source of these devices constrain their assisting duration and make them remarkably dependent on their battery life [118]. The review published by Young and Ferris [36] reported that the maximum functioning duration of portable exoskeletons is 5 hours indicating several recharging requirements in a day. Harvesting the dissipated energy of assistive devices can address this issue on the mobile exoskeletons and help users to be more independent by prolonging the device battery life [118–120]. The regenerating and harvesting energy has been utilized in different assistive devices to improve the efficiency of the device that has been excellently reviewed in several review papers [118–120].

The regeneratable power of the optimal exoskeletons can be acquired by capturing the negative power profiles of assistive actuators and obtaining the dissipated energy from the negative power profile. This dissipated energy was normalized by the mass and gait duration of each subject and trial and reported by averaging within trials of each subject. Although the maximum efficiency of harvesting dissipated power is ranged between 30% to 37% for the lower limb assistive devices [118], the MIT cheetah custom design [121, 122] and the biomechanical energy harvester developed by Donelan et al. [123] reported and experimentally verified 63% regeneration efficiency. Hence, we selected 65% as energy harvesting efficiency for the analyzed exoskeletons which is the maximum efficiency that has been reported for regeneration. The regeneration effect on the simulated configurations of devices and their optimal trade-off has been studied by subtracting the regenerable power from the total power consumption of devices. This analysis has been performed on the subjects walking at free speed without carrying any external load to conduct some further investigations on the effect of devices inertial properties and regeneration on both metabolic and device power consumption.

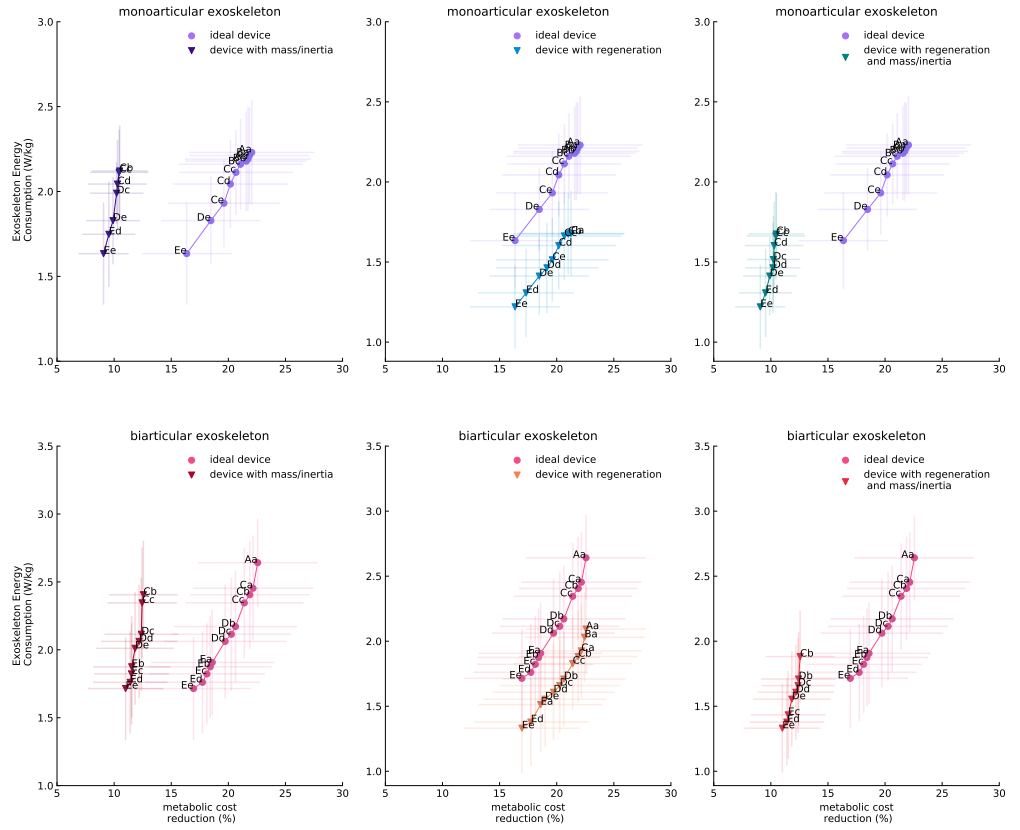


Fig 14. Pareto front of devices in ideal condition and under regeneration and device mass and inertia effects. The label on each marker is denoted to results from different peak torque constraints. The hip and knee constraints are labeled from *A* to *E* and *a* to *e* respectively. The *A*, *a* to *E*, *e* labels represent for 70 N.m to 30 N.m constraints respectively, and each marker, which stands for a specific configuration of a device, is labeled by the hip and knee constraints labels. The optima points on Paretofronts are resulted from averaging over 7 subjects walking in *noload* condition.

The effect of devices inertial properties on the simulated devices are remarkable, and this effect changes most of the devices on the optimal trade-off curve, as represented in figure 14. The highest peak torque in both monoarticular and biarticular exoskeletons are 60 N.m for the knee and 50 N.m for the hip joint. Since the inertia of devices was getting affected by altering the peak torque, results indicating that the reflected inertia have a considerable effect on the optimality of the devices and power consumption of exoskeletons with high peak torque is not efficient in comparison to the amount of metabolic cost reduction they provide.

While the biarticular exoskeleton showed better performance than monoarticular when the exoskeletons inertial properties were considered (Fig. 15), the slope of Pareto front for both exoskeletons indicates that devices with higher torque capacity will not make a considerable change on the amount of assist that device can provide to the subjects due to the inertia and this effect can be seen more obviously for the monoarticular device.

The energy harvesting had a remarkably positive effect on the devices, and it enabled some new configurations in both devices to become optimal in the amount of

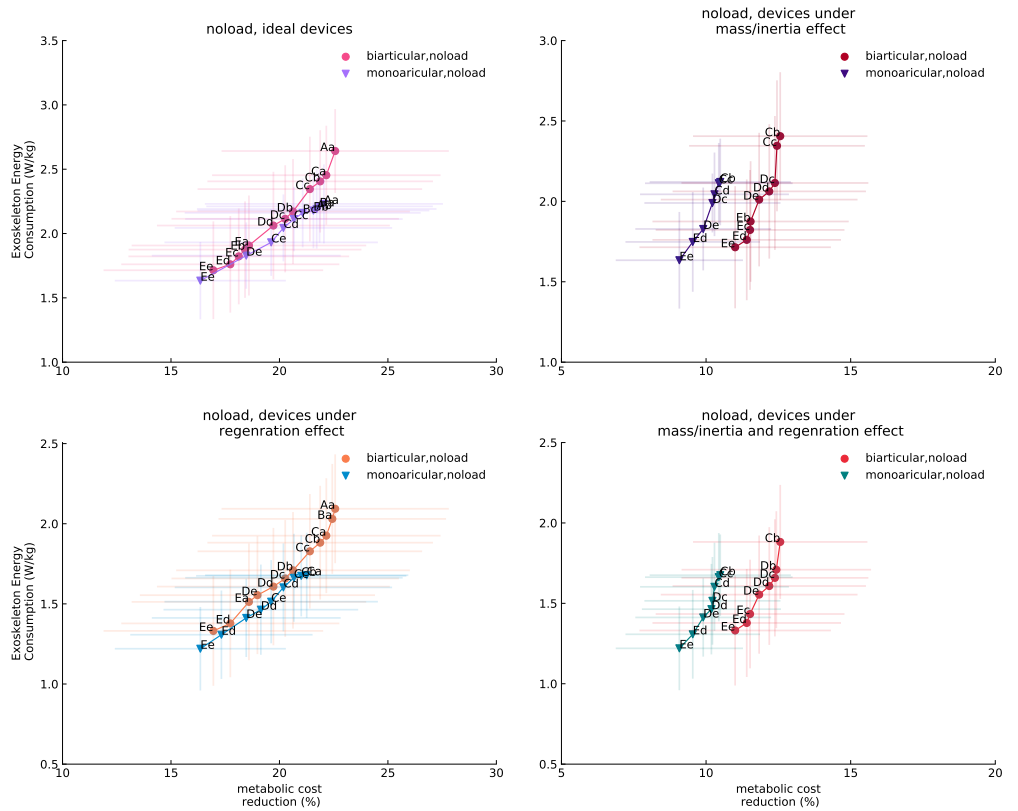


Fig 15. The comparison of the pareto fronts of devices in different metabolic and device power expenditure conditions. The biarticular and monoarticular exoskeletons have been compared in (a)ideal condition, (b)under devices mass/inertia effect on metabolic energy consumption, (c)under dissipated energy regeneration effect on power consumption of devices, and (d)under the effect of (b) and (c). The optima points on Paretofronts are resulted from averaging over 7 subjects walking in *noload* condition.

power consumption for delivered assistance, as shown in figure 14and 15. The changes in Pareto front of biarticular and monoarticular exoskeletons show that regenerating the dissipated power of devices can profoundly reduce the required power for actuating the exoskeleton. This energy requirement reduction enables the battery and mechanical designers to reduce the load on the musculoskeletal system of subjects, which causes metabolic energy consumption increase in the individual being assisted and requires the device to compensate for this increase ahead of providing assistance to the subject. Finally, analyzing both exoskeletons with inertia and mass and regeneration effect reveals that the exoskeletons have dramatically different performance than the ideal devices, as shown in figure 14 for subjects in *noload* condition. Unlike the ideal optimal trade-off, the biarticular device shows superior performance than the monoarticular exoskeleton (Fig. 15), and the exoskeletons under regeneration and mass and inertia effect have different optimal configurations than ideal condition.

The analyses accomplished for the effect of regeneration and devices inertial characteristics on the performance of assistive devices can provide a qualitative perspective for the mechatronic systems designers on designing assistive devices. The general outcome of these analyses shows that selecting an actuator with high torque density is essential to reduce the reflected inertia effect of gear train on the energy

expenditure of subjects. The active inertia compensation methods by designing a controller also can be helpful in reducing the impact of inertia on the metabolic expenditure increase of subjects, which has been used by [124] for controlling one degree of freedom knee exoskeleton to compensate its inertia; however, this method comes with some coupled stability issues [124–126] that need to be addressed while designing the controller.

The results also showed that keeping the actuator mass near to proximal joints and assisting the joint of interest distally has a considerable impact on the metabolic power consumption of subjects. As we discussed previously, this mechanical design conclusion has already been studied on the human musculoskeletal system, and it is shown the biarticular muscles enable human musculoskeletal structure to keep muscle volume near to trunk and transfer energy to the distal joints to reduce the inertia and mass of the leg. Consequently, the bio-inspired biarticular and multiarticular configurations of the assistive devices can provide a promising improvement in their performance.

Although assistive design with highly effective regeneration requires system-level optimization and complicating the design of assistive devices [118], even a qualitative comparison between devices with and without regeneration shows a remarkable difference in energy consumption. This implies the necessity of regeneration, especially for untethered devices, to improve their independence and their operation duration.

Case Study

We conducted four different case studies to get more insight into the performance of assistive devices that include studying both assistive devices in a particular load condition or an assistive device in two different load conditions with the same effect on the metabolic energy expenditure or the same energy consumption of assistive actuators. Investigating these specific configurations of the optimal devices helped us to understand how the profiles of devices with the same performances are changing in a load condition more systematically. These cases can clarify the effect of load condition on an assistive device profiles, and their muscles and how a particular device will be affected by loading assisted subjects with a heavy load.

Modified Augmentation Factor. In the case studies, we need to have a more systematic analysis of the performance of devices that can be employed for both *loaded* and *noload* conditions. Consequently, we used augmentation factor [41] with some primary modifications.

The augmentation factor (AF) was developed by Mooney et al. [41] to address the limitations of the performance index introduced by Sawicki and Ferris [127] to measure the relationship between the device applied positive power and change in metabolic power consumption. The augmentation factor established to estimate metabolic power change due to carrying the exoskeleton which balances between the mean positive power, resulting in a metabolic improvement and net dissipated power and device weights, causing metabolic detriment.

Although the augmentation factor resolves the previous performance metrics difficulties and introduces a general factor for predicting the performance of assistive devices, it does not account for the effect of inertia caused by the actuation unit and attached masses in moving segments. The study accomplished by Browning et al. [114] and our analysis on the effect of inertia and mass on the metabolic power change in the previous section noted the importance of the inertia effect on the metabolic burden of subjects showing the necessity of including this factor for any performance measurement of exoskeletons.

The modified augmentation factor (MAF) has been introduced to address this

central issue on the augmentation factor. In order to include the inertia effect on the augmentation factor, we adopted the model developed by Browning et al. [114] for estimating the metabolic power ratio change due to inertia ratio change of subjects walking while wearing weights on their lower limbs to subject walking without any load. Then, we performed some simple algebraic manipulations to obtain the device location factor (γ_i) for the applied inertia to each segment as it is represented in Eqn.(21). It is noteworthy to mention that γ_i is obtained under the assumption of device inertia addition to the inertia of unloaded leg.

$$\gamma_i = \frac{A_i \times m_{subjects} \times MC_{unloaded}}{I_{unloaded}} \quad i \in \{1, 2, 3\} \quad (21)$$

In this inertia position factor represented in Eqn.(21), A_i is the multiplier of I_{ratio} in Browning models for foot, thigh and shank segments and $I_{unloaded}$, $m_{subjects}$, and $MC_{unloaded}$ are the inertia of leg without any external load, mean weight of subjects, and metabolic rate of subjects walking without any load on their segments respectively which were obtained from the [114] models and plots. The modified augmentation factor (MAF) has been obtained by adding the effect of inertia on the metabolic detriment part of this factor, and it can be expressed as Eqn.(22).

$$MAF = \frac{p^+ + p^{disp}}{\eta} - \sum_{i=1}^4 \beta_i m_i - \sum_{j=1}^3 \gamma_j I_j \quad (22)$$

$$p^{disp} = \alpha(p^- - p^+) \quad \alpha = \begin{cases} 1 & p^+ < p^- \\ 0 & p^+ \geq p^- \end{cases} \quad (23)$$

Where p^+ , p^- , and p^{disp} is representing mean positive, negative, and dissipated power that is calculated through Eqn.(23). The β_i in MAF stands for the device mass location factor which is 14.8, 5.6, 5.6, and 3.3 W/kg from the foot to waist respectively [41, 114] and γ_j is representing device inertia location factor which is 47.22, 27.78, and 125.07 $W/kg.m^2$ from the foot to thigh respectively. Consistent with augmentation factor procedure [41], MAF uses muscle-tendon efficiency, $\eta = 0.41$ to convert the mechanical assistive power to metabolic power determined empirically by Sawicki and Ferris [127] and Malcolm et al. [40]. Finally, we normalized modified augmentation factor by the weight of each subject and averaged over the trials for each subject to reduce the deviation of this factor within subjects.

Root mean square error of profile in gait phases. Thus far, any comparison between the two power, torque, or speed profiles was a qualitative comparison. However, establishing a quantitative comparison between two selected profiles can be a more informative and systematic comparison. To this end, phases of a general gait cycle were adopted from [128] and customized for each subject and trial according to their toe-off timing, as it is represented in figure in S1 Fig. Then, the gait cycle of each subject and trial was partitioned to its phases, and we used the root mean square error (RMSE) method to compute the difference between two profiles in each phase of the gait cycle, and the calculated differences for each phase were averaged within trials for each subject.

Case 1: Devices Performance in *loaded* Condition

It is shown that the optimal trade-offs of both exoskeletons are practically the same for *loaded* condition, and due to this issue, we selected two devices on Pareto front that have almost the same performance in both metabolic cost reduction and power consumption. The chosen device for monoarticular has 70 N.m hip peak torque and 40 N.m knee peak

torque, which is represented by "Ad" on Pareto front (figure 10) and the peak torques of the biarticular device are 40, and 70 N.m on hip and knee respectively represented with "Da" on the Pareto front. As it can be inferred from the configurations of devices, although these two devices have the same performance on defined objectives, they have a completely different arrangement on hip and knee actuators. The metabolic rate of

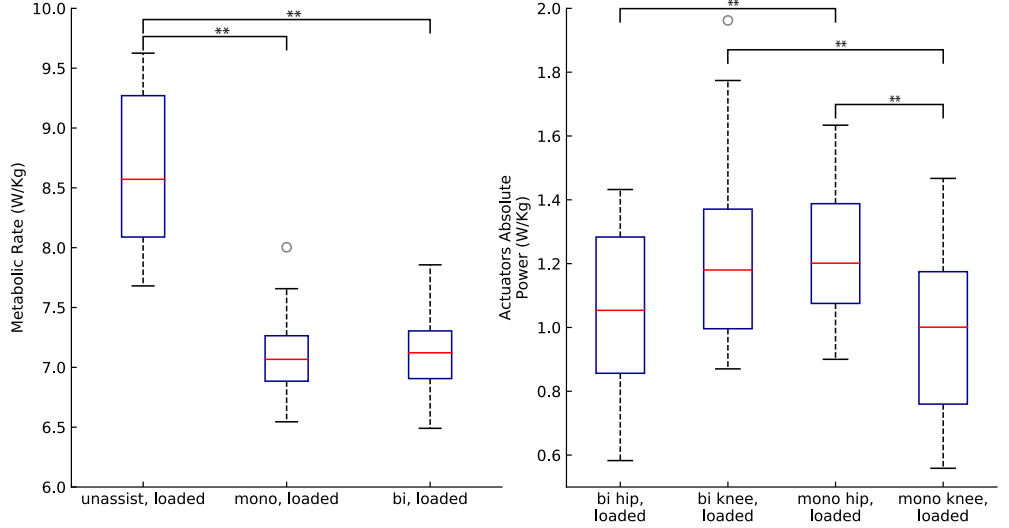


Fig 16. Assistive devices power consumption and its effect on the metabolic rate. The power consumptions of assistive devices and their effect on whole-body metabolic rate of the subjects walking at self-selected speed while carrying a heavy load. Asterisks indicate statistically significant differences (7 subjects, 3 trials, Tukey Post-hoc, $P < 0.05$).

assisted subjects with biarticular and monoarticular devices shows that there is no significant difference between the amount of assistance delivered by these devices, which was expected from the Pareto front. While the total power consumptions of these two devices are practically identical on the Pareto front, the power rate of hip and knee between biarticular and monoarticular devices are statistically significantly different as it is represented in figure 16. This difference indicates that while they have the devices deliver an equal amount of assistance to the subjects with a heavy load, their assistance strategies are different, which can be illuminated by analyzing the profiles of actuators.

The overall trend between torque profiles of the monoarticular and biarticular devices is similar, which can be seen in figure 17 qualitatively, and root mean square error between the profiles during the whole gait cycle can also proof this quantitatively claim as shown in figure 18. The detailed analysis of the gait cycle shows that the main difference between torque profiles of hip actuators is occurring during the stance phases and monoarticular deliver more hip extension torque than the biarticular device, especially during the mid-stance and terminal-stance phases (Fig. 17 and 18). Although the difference between profiles of hip actuators follow similar trajectories during the swing phase, the terminal-swing phase of these actuators is considerably different in which monoarticular deliver extension while biarticular provide flexion torque to the joint.

Although the biarticular and monoarticular knee actuators have an almost identical trajectory during the swing phase as their RMSE also shows in figure 18, there are some significant differences between these two actuators during the stance phases. While the biarticular knee actuator opposes with the torque generated by muscles around the knee joint during all stance phase, the monoarticular knee actuator assists the knee muscles

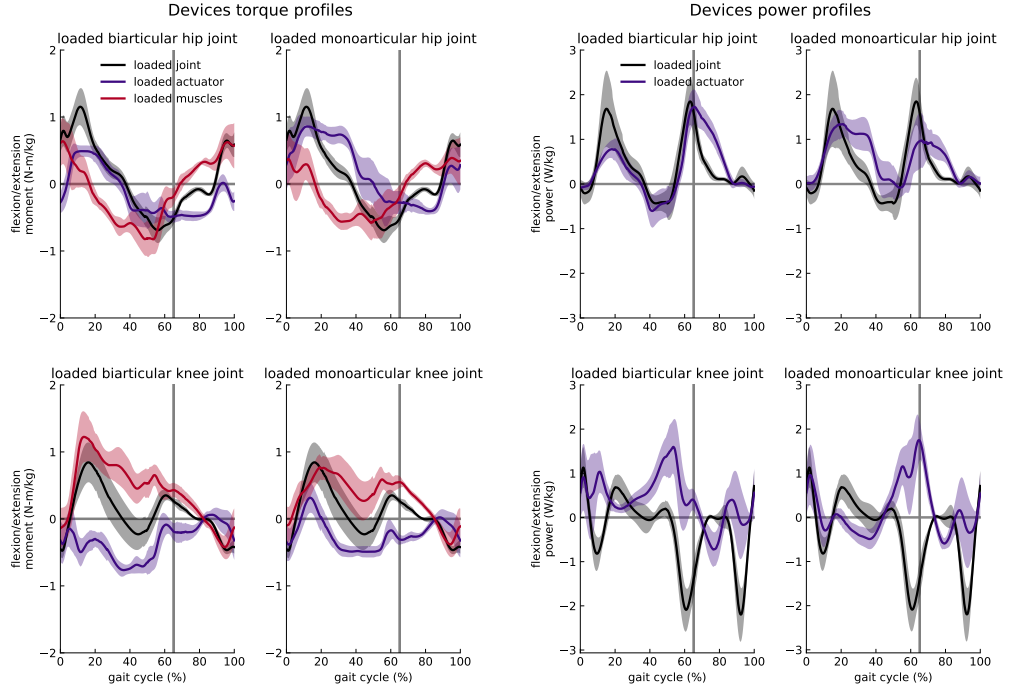


Fig 17. Assistive devices torque and power profiles. The actuator torque and power for subjects carrying heavy load (dark blue), and net joint power profile for *loaded* (black) condition are shown for each actuator of the devices. The curves are averaged over 7 subjects with 3 trials and normalized by subject mass; shaded regions around the mean profile indicate standard deviation of the profile.

generated torque during the loading response and mid-stance phases.

These remarkable differences between torque profiles of two devices affect the torque trajectories generated by muscles around the knee and hip joints, indicating muscular activation differences between subjects assisted by monoarticular and biarticular exoskeletons, nevertheless, according to the root mean square error between hip and knee muscles generated torque trajectories, the differences are not substantial except on the loading phase of the knee joint.

The comparison between the muscular activation of the *loaded* subjects assisted by ideal devices and constrained devices indicates substantial differences in some muscles. The activation of rectus femoris and psoas as two primary muscles on the hip and knee are considerably different between these two conditions, which can also explain the significant part of the difference between the muscle activations. This difference is not only between the ideal and constrained device but also the constrained biarticular, and monoarticular exoskeletons have a different impact on these two muscles (S2 Fig), which can roughly explain the variation between the muscles generated moment. Another remarkable difference between the ideal and constrained devices can be seen in gastrocnemius medial head muscle, where the activation of this muscle has been increased during the loading response to terminal stance phases. Since the activation of the gastrocnemius muscle increased, it can provide more moment on the ankle as well, and the activation of the soleus does not need to be increased considerably to compensate for the inadequacy of the moment generated by gastrocnemius. The muscular activation of subjects assisted by monoarticular and biarticular constrained devices are not limited to rectus femoris and psoas muscles, but the other representative

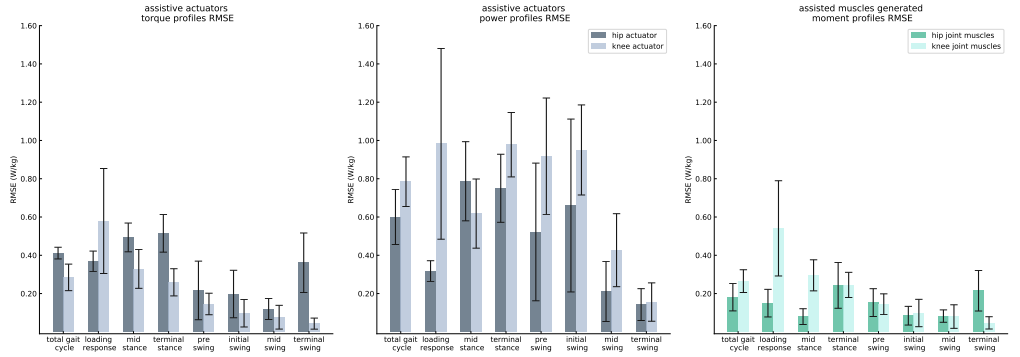


Fig 18. Assistive devices torque and power and muscles generated moment profiles root mean square error. The root mean square error between actuators of biarticular and monoarticular devices and the muscles generated moment of subjects assisted by these devices.

muscles show some differences as it is shown in the figure in S2 Fig nevertheless, the differences between them are not as considerable as rectus femoris and psoas muscles.

Unlike the moment profiles of devices where the difference was significant only in some specific phases, the power profiles of the biarticular and monoarticular devices have significant differences as it is shown qualitatively and quantitatively in figure 17 and 18 respectively. The difference between the power profiles of these two dives is more notable in the knee actuator in which the devices follow different trajectories during the gait cycle. Similar to the knee actuators, the hip actuators also have roughly different power profiles, and their maximum power consumptions occur in two completely different phases, similar to the knee actuators. The difference between the trajectories and magnitudes of the power profiles also can explain the statistically significant difference observed between the monoarticular and biarticular exoskeletons (Fig.16).

Unlike the moment profiles of devices where the difference was significant only in some specific phases, the power profiles of the biarticular and monoarticular devices have significant differences as it is shown qualitatively and quantitatively in figure 17 and 18 respectively. The difference between the power profiles of these two dives is more notable in the knee actuator in which the devices follow different trajectories during the gait cycle. Similar to the knee actuators, the hip actuators also have roughly different power profiles, and their maximum power consumptions occur in two completely different phases, similar to the knee actuators. The difference between the trajectories and magnitude of the power profiles also can explain the statistically significant difference observed between the monoarticular and biarticular exoskeletons.

Although the selected monoarticular and biarticular exoskeletons have the same effect on the metabolic rate of *loaded* subjects, it is already shown that their assistive actuator configurations are different which resulted in significantly different power rate of actuators. This difference in the configuration of their actuators affects their mechanical design, especially their required gear train and reflected inertia consequently. We employed the developed modified augmentation factor to assess the performance of the biarticular and monoarticular exoskeletons under the effect of device inertial properties. The computed modified augmentation factor for monoarticular and biarticular was 0.66 ± 1.00 and 1.98 ± 0.71 W/kg, which indicates that both exoskeletons would be able to deliver assistance to the subjects even under inertial properties of devices causing more metabolic burden on the subject. Additionally, the MAF shows that biarticular device has superior performance than monoarticular

exoskeleton and the reason for this issue embedded on the mass distribution and gear train of the monoarticular device. The inertia calculations show the device has practically three times more inertia on the thigh than the biarticular device and, according to Eqn.(22) and the inertia location factor of the thigh, the effect of inertia on the thigh is expensive in terms of the metabolic rate increase which results in a lower MA factor for the monoarticular exoskeleton.

Studying this specific case of monoarticular and biarticular devices proves the devices with the same total power consumption can have different power consumption in different joints. Additionally, it is shown that the optimal devices with the same performance can follow different moment and power profiles, even under kinematic similarities due to the arrangement of actuators. Although the devices were selected from the ideal Pareto front with the same performance, employing the modified augmentation factor for the monoarticular and biarticular devices with different mass and inertia characteristics indicated the superior performance of the biarticular device. It emphasizes the discussion held in the Mass, inertia, and regeneration effects section that biarticular device could deliver the same amount of assistance to the subjects more effectively than the monoarticular configuration.

Case 2: Devices Performance in *noload* Condition

In the second case study, we selected two devices with different power consumptions and the same effect on the metabolic rate of subjects walking without any extra load, which are shown with "*C_b*" and "*B_a*" on the biarticular and monoarticular Pareto front of the *noload* condition. Although the total performance trade-off of these two biarticular and monoarticular devices are different in mean values, the statistical tests on the mean absolute power consumption of actuator showed no statistically significant difference between actuators of the monoarticular and biarticular exoskeletons. The power

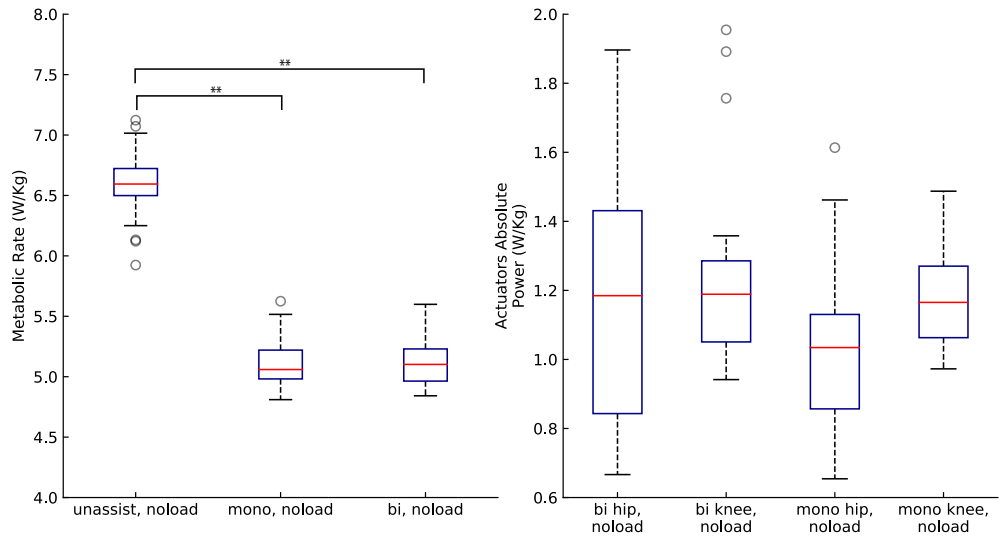


Fig 19. Assistive devices power consumption and its effect on the metabolic rate. The power consumptions of assistive devices and their effect on whole-body metabolic rate of the subjects walking at self-selected speed without any additional load. Asterisks indicate statistically significant differences (7 subjects, 3 trials, Tukey Post-hoc, $P < 0.05$).

consumption of hip actuators in both exoskeletons had a high within-subject deviation, as it is shown in figure 19, which may explain the absence of a statistically significant

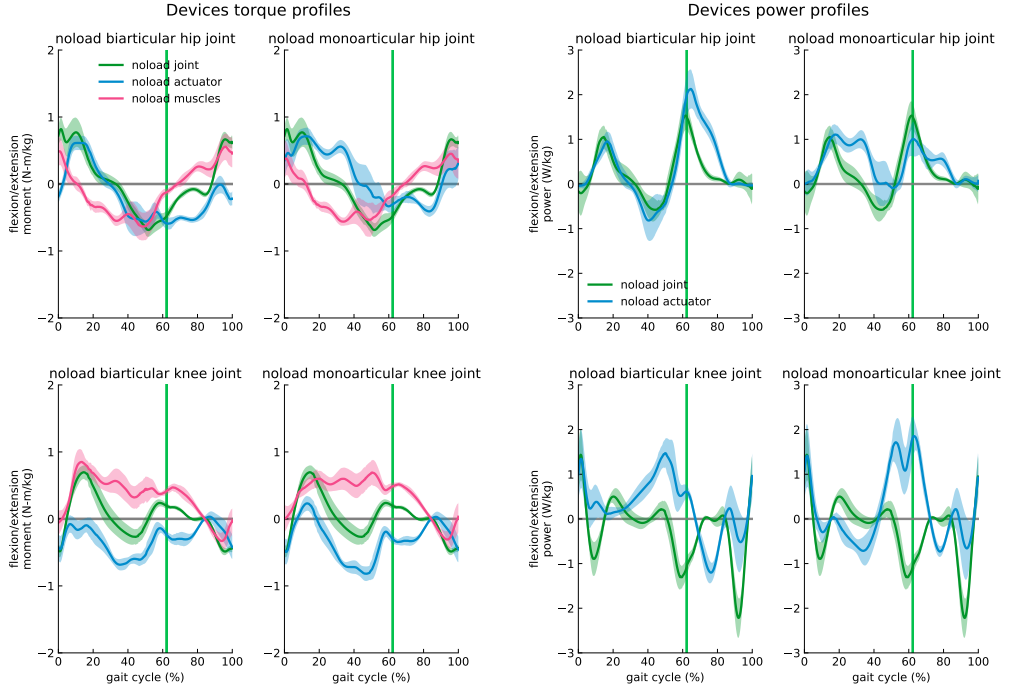


Fig 20. Assistive devices torque and power profiles. The actuator torque and power for subjects carrying heavy load (dark blue), and net joint power profile for *loaded* (black) condition are shown for each actuator of the devices. The curves are averaged over 7 subjects with 3 trials and normalized by subject mass; shaded regions around the mean profile indicate standard deviation of the profile.

difference between the actuators. Additionally, the metabolic rate of subjects assisted with monoarticular and biarticular devices has no significant difference; still, the metabolic rate reduction caused a significant difference between the unassisted and assisted subjects, as represented in figure 19.

The analysis of moment profiles of assistive devices in the *noload* condition shows that the differences between these two devices are similar to the difference of biarticular and monoarticular devices in the *loaded* circumstance which is represented in figure 20. Nevertheless, the variations of moment generated by muscles of assisted subjects are negligible in *noload* condition (Fig. 21), which signals identical muscular activation of subjects assisted with these exoskeletons. Unlike the moment profiles, the power profiles of the devices are different in *noload* condition, unlike the moment patterns. It can be seen from the power profiles that devices follow notably different trajectories during a gait cycle to deliver assistance to the subjects and these profiles in the hip actuators, similar to the knee actuators, have the highest contrast during the pre-swing phase according to their RMS error shown in figure 21.

Despite the large variation between the power consumption of the devices and the absence of significant difference among their actuators, employing the modified augmentation factor indicates the remarkably different performance for monoarticular and biarticular exoskeletons on delivering assistance to the subjects. The selected devices have a different design in the actuators in which the biarticular device can provide maximum 50 and 60 N·m/kg torque in hip and knee actuators respectively; yet, the maximum providable moments in the hip and knee actuators of the monoarticular device are 60 and 70 N·m/kg respectively. The computation of MAF under described

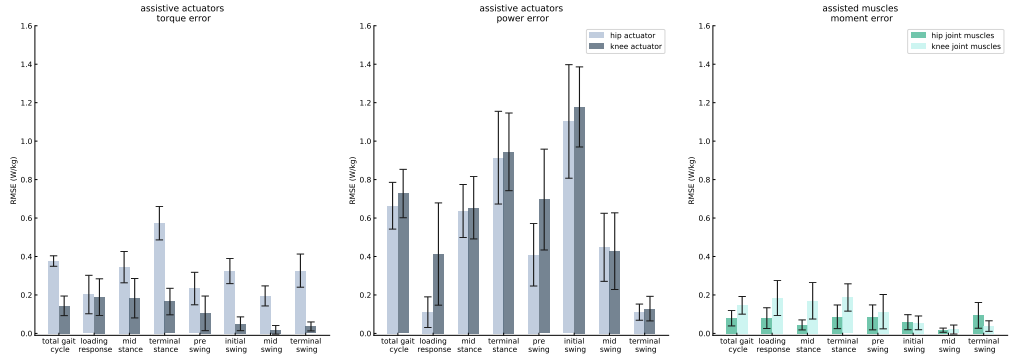


Fig 21. Assistive devices torque and power and muscles generated moment profiles root mean square error. The root mean square error between actuators of biarticular and monoarticular devices and the muscles generated moment of subjects assisted by these devices.

configurations of devices resulted in 1.57 ± 0.72 W/kg and 0.42 ± 0.85 for biarticular and monoarticular devices indicating the better performance of the biarticular device similar to the first case. The performance of these two devices can also be discussed based on the Pareto front of devices under inertia and mass effect shown in figure 15. According to this analysis (Fig. 15), the studied configuration of the monoarticular device became a nondominant solution in Pareto simulations under the inertial properties of devices, while the chosen biarticular device could maintain its efficiency under the negative effect of its inertial properties on the metabolic rate of subjects. This analogy between the Pareto front with devices inertial properties effect consideration and MAF can also confirm the extension of the augmentation factor.

Studying specific optimal monoarticular and biarticular exoskeletons in two load conditions which were chosen from the Pareto fronts show that the even though the devices have practically the same performance in the optimal trade-off between the device total power consumption and metabolic cost reduction curves, their provided moment during a gait cycle has considerable differences which can have a different effect on the muscular activation of assisted subjects as well. These two case studies also show that the power profiles of monoarticular and biarticular devices are considerably different, though they have a similar total power consumption.

The study on the performance of selected devices in both loading conditions by developed MAF factor supports the discussion held on the "Mass, inertia and regeneration effects" section on the effect of the mechanical design on the performance of devices and also showed that the performance of the monoarticular exoskeleton highly affected with the inertial properties of the device. Although the mechanical design of a biarticular device can be complicated, its performance under the device inertial properties seems promising in both loading conditions according to the performance of studied cases (MAF value). The studied cases and general Pareto front of monoarticular device under its inertial characteristics effect show that the monoarticular device needs to be designed thoughtfully to reduce the effect of inertia and mass effect of the device on the metabolic burden of subjects complicating the design procedure and ignoring the mechanical design may result in delivering no assistance to the subject or increasing their metabolic burden. Even if the device with poor mechanical design can deliver assistance to the subjects, it will be costly in terms of power consumption.

Case 3: Biarticular Exoskeleton Performance

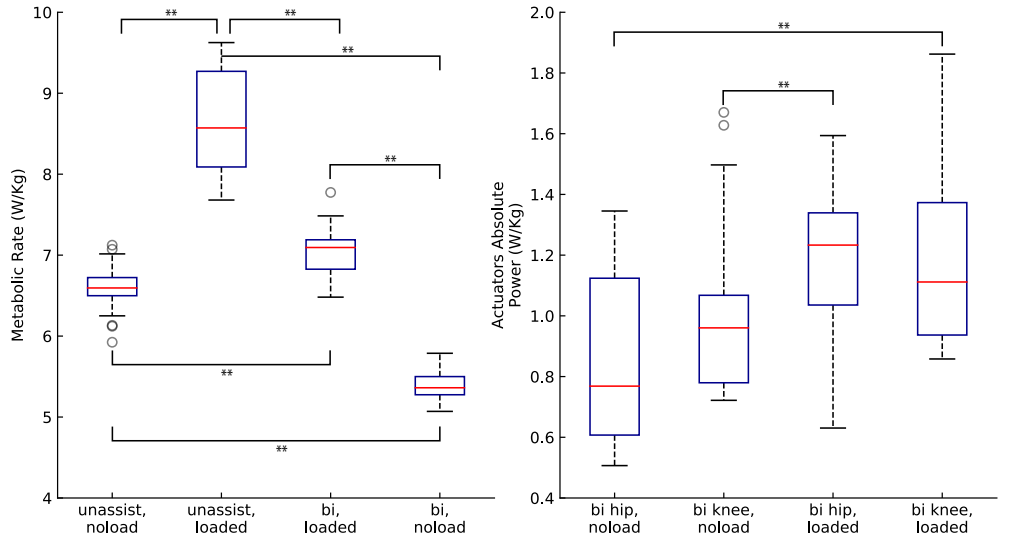
To study how the performance of the biarticular exoskeleton changes by loading subjects with a heavy weight on torso more specifically, we chose two cases in which the biarticular exoskeletons had the same effect on the metabolic rate of subjects in one case, and they had the same power consumption in another case. The selected configuration of the biarticular exoskeleton in *noload* condition is "*Ec*" with 30 and 50 N-m/kg peak torque in the hip and knee actuators, and it was compared to the same configuration (i.e., "*Ec*") in *loaded* condition where they had practically the same power consumption according to figure 10. For conducting the comparison with the likewise metabolic burden reduction, the same configuration of *noload* condition (i.e., "*Ec*") was compared to the biarticular exoskeleton with 50 and 60 N-m/kg peak torque in the hip and knee actuators represented by "*Cb*" on the Pareto front of the *loaded* biarticular exoskeleton.

The comparisons of the metabolic rate of assisted subjects by the biarticular device in two similar metabolic reduction and power consumption conditions have been represented in figure 22. The metabolic rate of subjects in both conditions shows that even though the metabolic rate of loaded subjects reduce considerably, there is a statistically significant difference between subjects walking normally and subjects assisted by the biarticular device in the *loaded* condition. The power consumption of the hip actuator, as well as the knee actuators in both loading conditions, showed no significant difference when the selected device was consuming a similar amount of power in both loading conditions; nevertheless, we observed a significant difference between the knee and hip actuators in different load conditions as shown in figure 23(b). Additionally, a similar performance in power consumption of two different configurations of the biarticular exoskeleton delivering a similar amount of assistance in different load conditions has been observed, which is represented in figure 23(a).

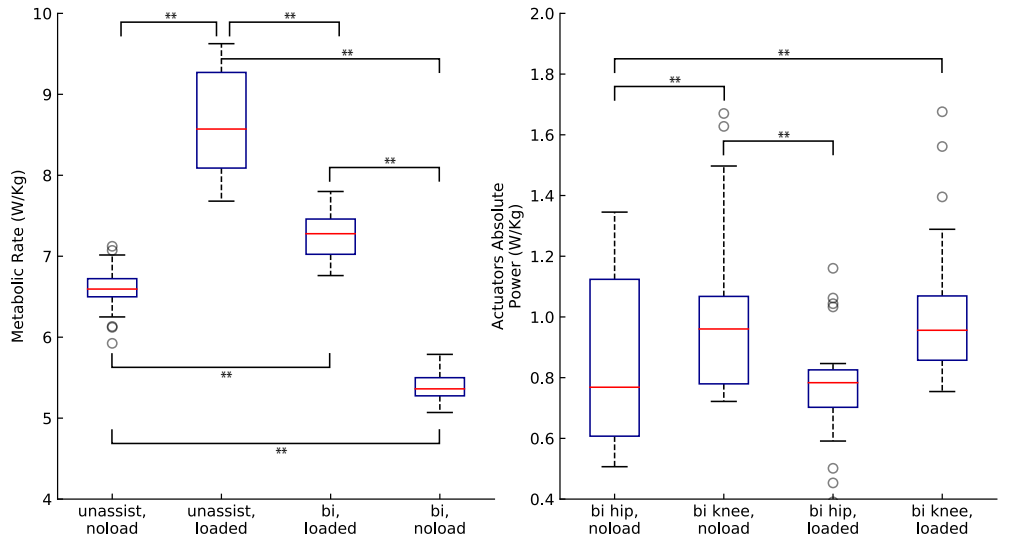
The absence of a significant difference between two devices with different configurations and different load conditions can facilitate designing a battery with a robust performance in different load conditions, and also this performance can help to have a general mechanical design for an exoskeleton to assist subjects in different load and assistance level conditions. Nevertheless, the high deviations and outliers of power consumption indicate high contrast within subjects that can complicate obtaining general power profiles for the device.

The performance assessment of the same biarticular configuration in two different load conditions by employing MAF showed that the performance of the biarticular exoskeleton in *loaded* condition was improved (1.40 ± 0.80 W/kg) in comparison with the *noload* condition where MAF was 1.01 ± 0.70 W/kg. Although the increase in the positive power of the device in *loaded* condition was expected, MAF improvement shows that this increase in positive power was delivered to the subjects effectively. In the meanwhile, comparing the devices with the same effect on the metabolic cost reduction of subjects in different load conditions showed superior performance of the biarticular device in the *loaded* in which devices in *loaded* and *noload* circumstances had 2.08 ± 0.69 and 1.01 ± 0.69 W/kg MAF value which can indicate inefficiency of *noload* device power profiles in general.

The quantitative along with the qualitative analyses of power and moment profiles between pair of devices in defined comparison cases not only show a moderate variation between the torque profiles of the compared biarticular device but also the power profiles have considerably low diversity in different load conditions as it is shown in figure 23(a), 23(b), and figure in S3 Figure supporting our claims on the high resemblance between profiles of the biarticular exoskeletons in loaded and *noload* conditions. As it is shown in figure in S3 Figure, the difference between the power and moment profiles of pair of devices in *load* and *noload* conditions are practically limited to the magnitude and timing based on the toe-off difference except on the pre-swing



(a) Biarticular exoskeleton with the same effect on the metabolic consumption of subjects



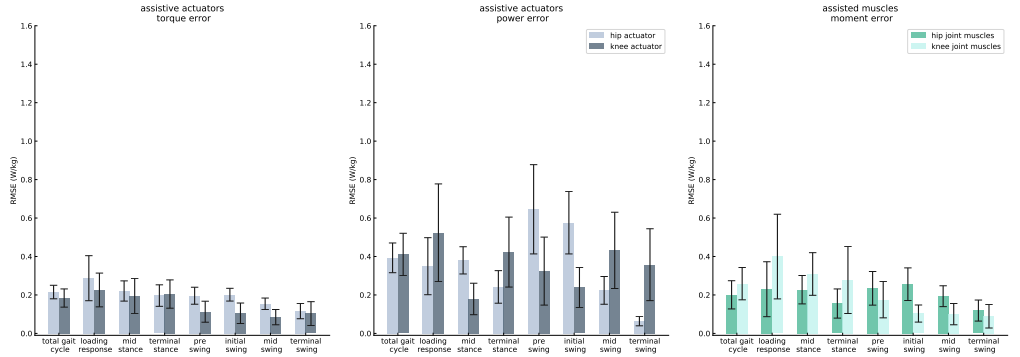
(b) Biarticular exoskeleton with the same total power consumptions

Fig 22. Biarticular exoskeleton power consumption and its effect on the metabolic rate in different load conditions. The power consumptions of biarticular exoskeleton and their effect on whole-body metabolic rate of the subjects walking at self-selected speed in both *loaded* and *noload* condition. Asterisks indicate statistically significant differences (7 subjects, 3 trails, Tukey Post-hoc, $P < 0.05$).

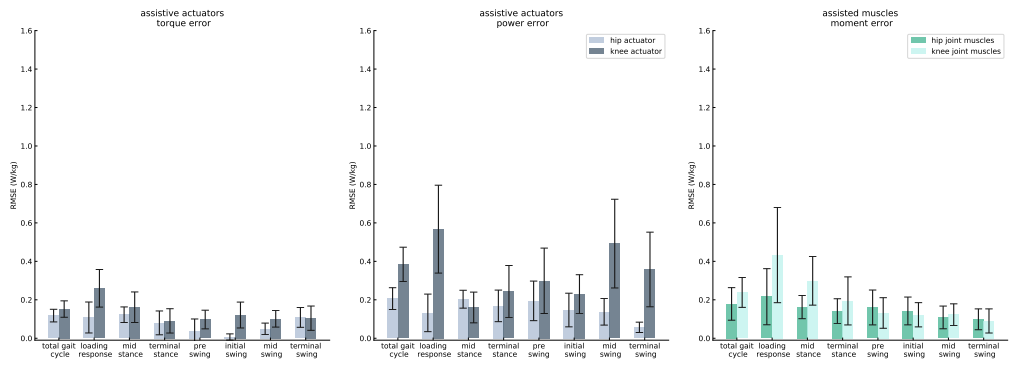
and initial-swing phases of knee profiles where the trajectories have rough differences between biarticular devices with the same effect on the metabolic power consumption of assisted subjects.

Case 4: Monoarticular Exoskeleton Performance

The same analyses on the biarticular exoskeleton in different load conditions, which was discussed in the previous case study, were performed on the monoarticular exoskeleton



(a) Biarticular exoskeleton with the same effect on the metabolic consumption of subjects



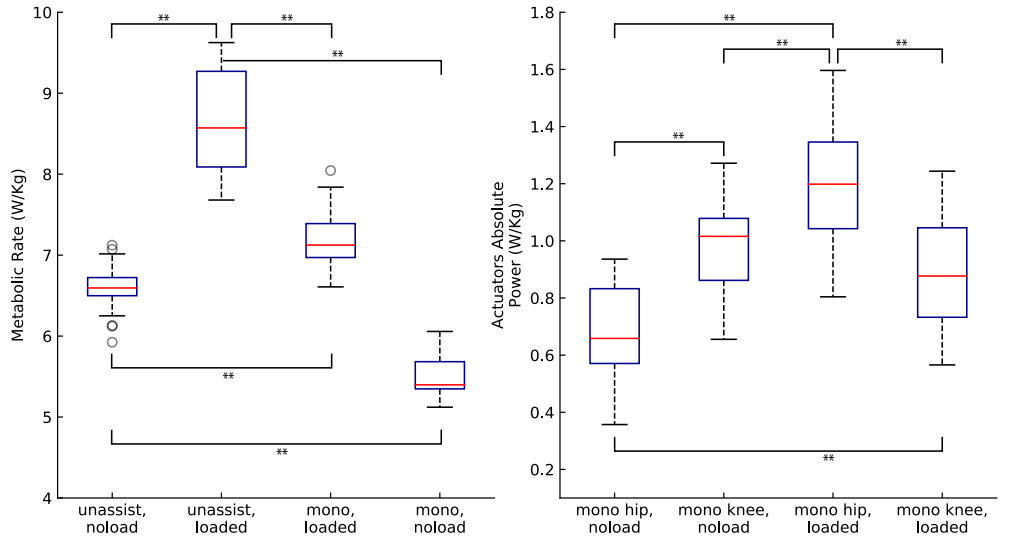
(b) Biarticular exoskeleton with the same total power consumptions

Fig 23. Biarticular exoskeleton torque and power and muscles generated moment profiles root mean square error in different load conditions. The root mean square error between actuators of the biarticular exoskeleton and the muscles generated moment of subjects assisted by this device *loaded* and *noload* conditions.

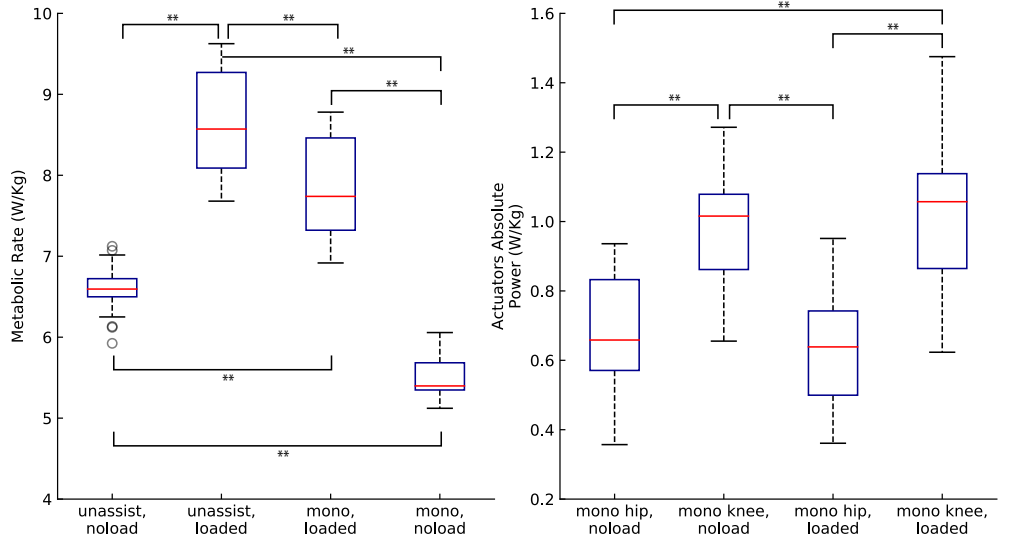
to get an in-depth insight into this device. To conduct the comparisons between a pair of monoarticular devices with a similar effect on the metabolic cost or with similar power consumption, we chose the *Ee* configuration of monoarticular in loaded and noload conditions and *Ae* monoarticular exoskeleton from the Pareto front of monoarticular in the loaded condition. The selected *Ee* and *Ae* configurations have 30 and 30N-m/kg and 70 and 30 N-m/kg peak torque constraints on the pair of hip and knee actuators.

The comparison of actuators power consumption between *Ae loaded* and *Ee noload*, which have a similar metabolic cost reduction, showed a notable increase in power consumption of the *loaded* hip actuator. Despite the reduction in the knee power consumption of *loaded* knee actuator, the difference between the pair knee actuators was not significant. One of the observed critical issues was that even though the within-subject variation of monoarticular devices was generally low, the divergence of actuators power consumption between the load condition and between the configurations was considerably high. As it is shown in figure 24(a) along with figure 24(b), while the power consumption of knee actuator in the low torque availability (i.e., *Ee*) was higher than the hip actuator, this was changed in higher torque constraints in which the hip became dominant power consumer that indicates considerable changes in the power profile of monoarticular device in different arrangements of its actuators.

The metabolic rate of the compared pairs of monoarticular devices has been shown in figure 24(a) and 24(b) that showed similar behavior observed in the previous case study; yet, it is noteworthy to mention the significant difference between the impact of



(a) Monoarticular exoskeleton with the same effect on the metabolic consumption of subjects

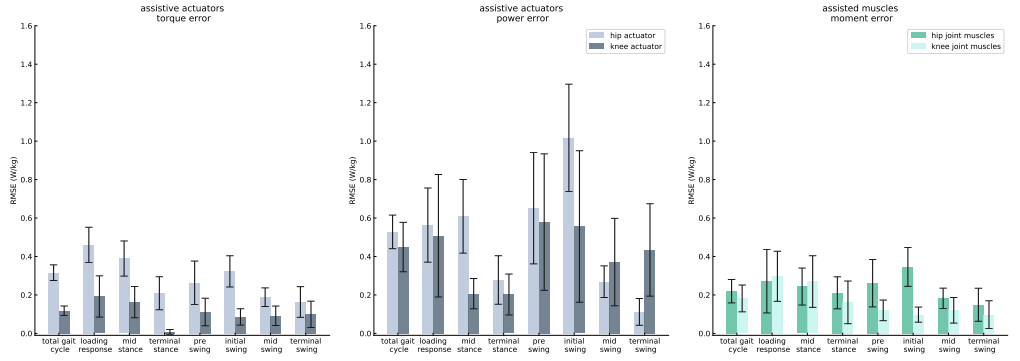


(b) Monoarticular exoskeleton with the same total power consumptions

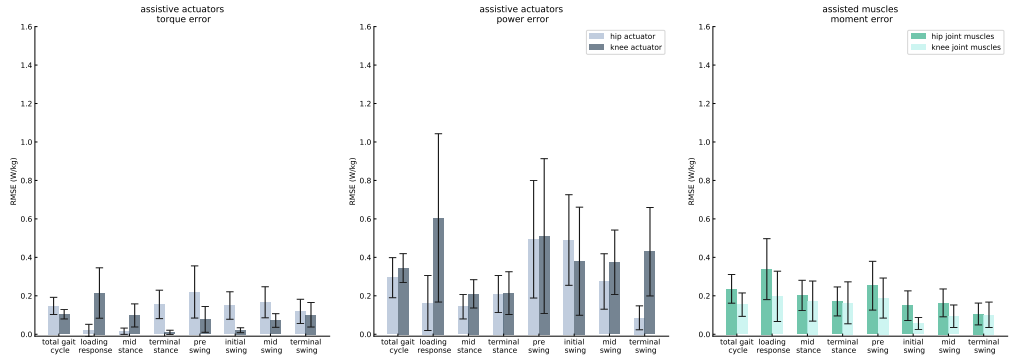
Fig 24. Monoarticular exoskeleton power consumption and its effect on the metabolic rate in different load conditions. The power consumptions of biarticular exoskeleton and their effect on whole-body metabolic rate of the subjects walking at self-selected speed in both *loaded* and *noload* condition. Asterisks indicate statistically significant differences (7 subjects, 3 trials, Tukey Post-hoc, $P < 0.05$).

Ee device on the metabolic burden reduction of subjects in different loading conditions that we did not observe in the biarticular case according to the Pareto front of a device in different load conditions as shown in figure10. These high deviations in both defined performance criteria can complicate obtaining a general exoskeleton that can deliver different levels of assistance with efficient power consumption.

The pair of devices selected for conducting the comparisons were evaluated by the modified augmentation factor to assess their performance under the mass and inertia effect. Unlike the other case studies in which all evaluated biarticular and monoarticular



(a) Monoarticular exoskeleton with the same effect on the metabolic consumption of subjects



(b) Monoarticular exoskeleton with the same total power consumptions

Fig 25. Monoarticular exoskeleton torque and power and muscles generated moment profiles root mean square error in different load conditions. The root mean square error between actuators of the biarticular exoskeleton and the muscles generated moment of subjects assisted by this device *loaded* and *noload* conditions.

devices were delivering a positive power to the human musculoskeletal system, the monoarticular exoskeletons evaluated in this case study both were causing an increase in the metabolic burden of subjects according to MAF performance factor. The modified augmentation factor of the monoarticular device with 30 N-m/kg peak torque constraints in both hip and knee actuators showed -0.20 ± 0.43 W/kg in the *noload* condition while it was increased to -0.15 ± 0.56 W/kg when subjects were loaded. These MAF values of the *Ee* monoarticular device represent a high variation of device effect on the subjects and improvement of the device performance by loading subjects, which was also observed in the biarticular exoskeleton. Even with the improvement of device performance in the loaded condition, the device in both load conditions would cause subjects to consume more power due to wearing these devices. The same analysis on the monoarticular device *Ae* configuration (70 N-m/kg hip 30 N-m/kg knee) in *loaded* condition showed relative improvement compared to the *Ee* device.

According to the MAF, the monoarticular exoskeleton require large torque capacity to deliver assistance to the subjects, and this observation is in contraction with our earlier claim about the monoarticular device in the *noload* condition under the inertial properties effect of devices. According to the slope of Pareto front of monoarticular device under the devices inertial properties effect, we claimed that it might be beneficial to keep the torque capacity of the monoarticular exoskeleton more moderate, yet, we observe in this case study that the monoarticular device cannot inject positive power to the human musculoskeletal system in low torque capacity, and this contraction might be

due to the differences between definitions of MAF and Pareto fronts under inertial effect which demands experimental justifications of defined performance criteria.

Although there are some quantitative divergences between the defined performance metrics, both Pareto front and MAF revealed the remarkably weak performance of monoarticular under device mass and inertia effect consideration. The MAF, along with Pareto front, supports our previous discussion regarding the monoarticular exoskeleton design and control and shows the necessity of inertia and gravity compensation for improving the efficiency of this device, which will lead to complex control architectures introducing several new challenges such as stability analysis, fundamental limitations, and other difficulties discussed in detail earlier.

The moment and power profiles of the selected monoarticular exoskeleton did not show a similar resemblance we observed in the biarticular device between the pair of actuators. The hip actuators of devices with the same metabolic reduction effect follow completely different trajectories, and it is not surprising that their power profiles have significant differences. Although the moment profiles of the knee actuators had a higher resemblance than the hip actuators, their power profiles showed relatively different paths during pre-swing and initial swing phases. The comparison of profiles in the same device (i.e., E_e) in different load conditions showed a considerable divergence between the moment and power profiles of hip actuator after the mid-stance phase of the gait cycle and their maximum difference have occurred during pre-swing and initial swing phases. The knee actuators showed a similar performance we already observed in another comparison condition in which even though the torque profiles of knee actuator in different load conditions were almost the same, their power profiles have remarkable differences during pre-swing and initial swing phases. These described moment and power profiles and their quantitative differences using RMSE in both comparison cases have been represented in the figure in S4 Figure and figure 25.

These variations on the profiles of the monoarticular device were already observed on the analysis of optimal devices torque and power profiles shown in figure 12 and 13. These case studies confirm our discussion about monoarticular exoskeleton in which we claim that obtaining a generic control profile for this device would be challenging and also the optimal battery design under its life and weight considerations, as optimality criteria, highly dependent on the selected configuration and a generic battery would not perform optimally for all devices.

Study Limitations

This simulation-based studying assistive device has some limitations that need to be considered for any interpretation of the results. One of the main limitations is kinematics and ground reaction forces for the assisted subjects; Although experimental studies reported that exoskeleton could make a minor [42, 84, 90, 129–131] and significant [85, 132–134] changes on assisted subjects kinematics and joint moment, our simulator's algorithm (CMC) is not capturing these changes and it is assumed that unassisted and assisted subjects have the same kinematics, ground reaction force, and joint moment, nonetheless, it is reported that metabolic cost may not substantially be affected by kinematics changes [135]. This limitation recently has been addressed by employing predictive simulations which can capture the changes in the kinematics and dynamics of the assisted subjects.

Secondly, as it is earlier stated, assistive devices that we modeled was assumed massless without any actuator and link mass and inertia; yet, in practice, exoskeleton actuation modules mass and their reflected inertia on the links are large and one of the main challenges on mechanical design of the exoskeletons and also it is proven that adding mass the lower limbs can considerably change metabolic cost of the subjects. The exoskeletons attachment on the body is also one of the central performance limiting

factors of the assistive devices [136] which is not modeled in ideal exoskeletons.

Another significant limitation of this study is limitations on musculoskeletal modeling. There are some influential restrictions on muscles modeling that affect the assistive devices simulations results. One of these restraints is extortionate passive force generated by the muscles [92], that can result in extortionate muscular activities which observed by similar work [93] when they were comparing simulation and experimental muscular activities. Another critical issue in Hill-type muscles modeling is that it does not take into account the muscle fatigue, which is an effective factor in muscle recruitment strategies [92]. Rectus femoris, which is more vulnerable to fatigue due to its fibers properties [137] was experiencing extreme activations in all of the assistance scenarios, which in practice may cause subjects muscles fatigue [138]. Tendon modeling, constant force enhancement, short-range muscle stiffness and some other factors [92] are limiting aspects of the muscles that affect the musculoskeletal models and the simulations results which need to be considered for any interpretation of this study's results.

We also would refer the readers to similar papers [2, 93], where they also discussed their studies limitation, which is similar in most of the aspects. Moreover, [92] provides comprehensive information about all aspects of the OpenSim simulations and propose some recommendation for any interpretation and validation of the simulations that can be beneficial to have an accurate interpretation of our results.

Conclusions and Future Work

In this study, we investigate how introducing biarticular configuration on assistive devices can affect the exoskeletons efficiency, assisted subjects muscles activity and their energy expenditure when running with 2 m/s speed by using musculoskeletal simulations. We introduced new configurations of the exoskeleton for knee and knee + Hip which can provide assistance with considerably higher efficiency in comparison with monoarticular configuration which can lead the exoskeleton design to get more effective assistive devices.

Thanks to musculoskeletal simulations we are given insight into how energy was consumed during a gait cycle and which phase of the gait exoskeletons require more energy and where we can harvest energy to charge the battery on untethered exoskeletons and also we could show that in lower energy consumptions, actuators power profile would not be effective for regeneration. This stage of the study can further help the designer to decide about the battery and its regeneration design. Taking advantage of the multi-criteria optimization concept to acquire the average Pareto front for each configuration enabled us to address how to compare different configurations of assistive devices while in different energy consumptions areas. This would help researchers and designers to simulate exoskeletons with their specifications such as energy consumption and torque requirement.

As future work, we will take into account the monoarticular and biarticular exoskeletons inertial properties which have been designed in our group to study our assistive devices effect on the running subjects energy expenditure, muscles activity and how adding inertia can affect the torque and power profiles. As it is discussed in the limitations of the study, global or dynamic optimization needs to be replaced by static optimization during the simulations which is called predictive simulation [96, 100] which will capture any ground reaction force, joint moment and kinematics changes and it should be one of the main future works for studying the exoskeletons effect on subjects suggested by the relevant researches [2, 93] as well. SCONE [139] is open-source software designed for performing predictive simulations of biological motion which can be used to study the assistive devices.

Simulations based on the Pareto front had limitations highlighted in the previous section, which should be addressed in future work. Infeasibility of the search and big discretization can be addressed by using normal boundary intersection method [110] which is designed for this purpose to resolve these issues on computationally heavy problems resulting in more accurate with lower discretization issue Pareto front for the subjects.

Simulations outcomes are beneficial as a prior information to assist the subjects, and they can be used on human in the loop optimization [140] as a prior profile to start optimization with the simulations torque profiles which may result in less optimization time by increasing convergence rate of the optimization; we will establish experimental setup and validate our simulations with inertial properties using experimental outcomes, then, human in the loop optimization may also examined using the simulations profiles in the next phases of this research.

Supporting information

S1 Fig. Phases of subjects gait in *noload* and *noload* conditions.

S2 Fig. Activation of nine representative muscles of *noload* subjects assisted by constrained devices (first case study).

S3 Figure. Biarticular exoskeleton torque and power profiles comparison between *noload* and *noload* conditions with the same power and metabolic consumptions (third case study).

S4 Figure. Monoarticular exoskeleton torque and power profiles comparison between *noload* and *noload* conditions with the same power and metabolic consumptions (fourth case study).

Acknowledgments

References

1. Rodman PS, McHenry HM. Bioenergetics and the origin of hominid bipedalism. American Journal of Physical Anthropology. 1980;52(1):103–106. doi:10.1002/ajpa.1330520113.
2. Uchida TK, Seth A, Pouya S, Dembia CL, Hicks JL, Delp SL. Simulating Ideal Assistive Devices to Reduce the Metabolic Cost of Running. PLOS ONE. 2016;11(9):1–19. doi:10.1371/journal.pone.0163417.
3. Carrier DR, Kapoor AK, Kimura T, Nickels MK, Satwanti, Scott EC, et al. The Energetic Paradox of Human Running and Hominid Evolution [and Comments and Reply]. Current Anthropology. 1984;25(4):483–495.
4. Fedak M, Pinshow B, Schmidt-Nielsen K. Energy cost of bipedal running. American Journal of Physiology-Legacy Content. 1974;227(5):1038–1044. doi:10.1152/ajplegacy.1974.227.5.1038.
5. Schalock RL. The concept of quality of life: what we know and do not know. Journal of Intellectual Disability Research;48(3):203–216. doi:10.1111/j.1365-2788.2003.00558.x.

6. Aoyagi Y, Shephard RJ. Aging and Muscle Function. *Sports Medicine*. 1992;14(6):376–396. doi:10.2165/00007256-199214060-00005.
7. Doherty TJ, Vandervoort AA, Brown WF. Effects of Ageing on the Motor Unit: A Brief Review. *Canadian Journal of Applied Physiology*. 1993;18(4):331–358. doi:10.1139/h93-029.
8. Brooks SV, Faulkner JA. 1994, Skeletal Muscle Weakness in Old Age: Underlying Mechanisms. *Sci Sports Exercise*;26:432–439.
9. Thelen DG, Schultz AB, Alexander NB, Ashton-Miller JA. Effects of Age on Rapid Ankle Torque Development. *The Journals of Gerontology: Series A*. 1996;51A(5):M226–M232. doi:10.1093/gerona/51A.5.M226.
10. Porter MM, Vandervoort AA, Kramer JF. Eccentric Peak Torque of the Plantar and Dorsiflexors Is Maintained in Older Women. *The Journals of Gerontology: Series A*. 1997;52A(2):B125–B131. doi:10.1093/gerona/52A.2.B125.
11. Vandervoort AA, McComas AJ. Contractile changes in opposing muscles of the human ankle joint with aging. *Journal of Applied Physiology*. 1986;61(1):361–367. doi:10.1152/jappl.1986.61.1.361.
12. Vandervoort AA, Chesworth BM, Cunningham DA, Paterson DH, Rechnitzer PA, Koval JJ. Age and Sex Effects on Mobility of the Human Ankle. *Journal of Gerontology*. 1992;47(1):M17–M21. doi:10.1093/geronj/47.1.M17.
13. Gajdosik RL, Vander Linden DW, Williams AK. Influence of age on concentric isokinetic torque and passive extensibility variables of the calf muscles of women. *European Journal of Applied Physiology and Occupational Physiology*. 1996;74(3):279–286. doi:10.1007/BF00377451.
14. DG T. Adjustment of Muscle Mechanics Model Parameters to Simulate Dynamic Contractions in Older Adults. doi: ASME; 2003.
15. Brown-Triolo DL, Roach MJ, Nelson KA, Triolo RJ. Consumer perspectives on mobility: implications for neuroprostheses design. *Journal of rehabilitation research and development*. 2002;39 6:659–69.
16. Farris DJ, Hampton A, Lewek MD, Sawicki GS. Revisiting the mechanics and energetics of walking in individuals with chronic hemiparesis following stroke: from individual limbs to lower limb joints. *Journal of NeuroEngineering and Rehabilitation*. 2015;12(1):24. doi:10.1186/s12984-015-0012-x.
17. Olney SJ, Richards C. Hemiparetic gait following stroke. Part I: Characteristics. *Gait & Posture*. 1996;4(2):136 – 148.
doi:[https://doi.org/10.1016/0966-6362\(96\)01063-6](https://doi.org/10.1016/0966-6362(96)01063-6).
18. Richards CL, Malouin F, Dean C. Gait in Stroke: Assessment and Rehabilitation. *Clinics in Geriatric Medicine*. 1999;15(4):833 – 856.
doi:[https://doi.org/10.1016/S0749-0690\(18\)30034-X](https://doi.org/10.1016/S0749-0690(18)30034-X).
19. Balasubramanian CK, Neptune RR, Kautz SA. Variability in spatiotemporal step characteristics and its relationship to walking performance post-stroke. *Gait & Posture*. 2009;29(3):408 – 414.
doi:<https://doi.org/10.1016/j.gaitpost.2008.10.061>.

20. Duncan PW, Sullivan KJ, Behrman AL, Azen SP, Wu SS, Nadeau SE, et al. Body-Weight-Supported Treadmill Rehabilitation after Stroke. *New England Journal of Medicine*. 2011;364(21):2026–2036. doi:10.1056/NEJMoa1010790.
21. Cruz TH, Lewek MD, Dhaher YY. Biomechanical impairments and gait adaptations post-stroke: Multi-factorial associations. *Journal of Biomechanics*. 2009;42(11):1673 – 1677. doi:<https://doi.org/10.1016/j.jbiomech.2009.04.015>.
22. Moriello C, Finch L, Mayo NE. Relationship between muscle strength and functional walking capacity among people with stroke. *Journal of rehabilitation research and development*. 2011;48 3:267–75.
23. Chen G, Patten C, Kothari DH, Zajac FE. Gait differences between individuals with post-stroke hemiparesis and non-disabled controls at matched speeds. *Gait & Posture*. 2005;22(1):51 – 56.
doi:<https://doi.org/10.1016/j.gaitpost.2004.06.009>.
24. Chen G, Patten C, Kothari DH, Zajac FE. Gait differences between individuals with post-stroke hemiparesis and non-disabled controls at matched speeds. *Gait & Posture*. 2005;22(1):51 – 56.
doi:<https://doi.org/10.1016/j.gaitpost.2004.06.009>.
25. Kubo K, Kanehisa H, Fukunaga T. Effects of resistance and stretching training programmes on the viscoelastic properties of human tendon structures in vivo. *The Journal of Physiology*;538(1):219–226. doi:10.1111/j.physiol.2001.012703.
26. Lichtwark GA, Wilson AM. Optimal muscle fascicle length and tendon stiffness for maximising gastrocnemius efficiency during human walking and running. *Journal of Theoretical Biology*. 2008;252(4):662 – 673.
doi:<https://doi.org/10.1016/j.jtbi.2008.01.018>.
27. Ruby BC, III GWL, Armstrong DW, Gaskill SE. Wildland firefighter load carriage: effects on transit time and physiological responses during simulated escape to safety zone. *International Journal of Wildland Fire*. 2003;12(1):111–116.
28. Knapik JJ, Reynolds KL, Harman E. Soldier Load Carriage: Historical, Physiological, Biomechanical, and Medical Aspects. *Military Medicine*. 2004;169(1):45–56. doi:10.7205/MILMED.169.1.45.
29. van Vuuren BJ, Becker PJ, van Heerden HJ, Zinzen E, Meeusen R. Lower back problems and occupational risk factors in a South African steel industry. *American Journal of Industrial Medicine*;47(5):451–457. doi:10.1002/ajim.20164.
30. Yagn N. Apparatus for facilitating walking, running, and jumping; 1890. Available from: <https://patents.google.com/patent/US420179A/en>.
31. Dollar AM, Herr H. Lower Extremity Exoskeletons and Active Orthoses: Challenges and State-of-the-Art. *IEEE Transactions on Robotics*. 2008;24(1):144–158. doi:10.1109/TRO.2008.915453.
32. Garcia E, Sater JM, Main J. Exoskeletons for Human Performance Augmentation (EHPA) : A Program Summary. *Journal of the Robotics Society of Japan*. 2002;20(8):822–826. doi:10.7210/jrsj.20.822.
33. Chu A, Kazerooni H, Zoss A. On the Biomimetic Design of the Berkeley Lower Extremity Exoskeleton (BLEEX). In: Proceedings of the 2005 IEEE International Conference on Robotics and Automation; 2005. p. 4345–4352.

34. Riener R, Lünenburger L, Maier IC, Colombo G, Dietz V. Locomotor Training in Subjects with Sensori-Motor Deficits: An Overview of the Robotic Gait Orthosis Lokomat. *Journal of Healthcare Engineering*. 2010;1(2).
35. Zeilig G, Weingarten H, Zwecker M, Dudkiewicz I, Bloch A, Esquenazi A. Safety and tolerance of the ReWalk™ exoskeleton suit for ambulation by people with complete spinal cord injury: A pilot study. *The Journal of Spinal Cord Medicine*. 2012;35(2):96–101. doi:10.1179/2045772312Y.0000000003.
36. Young AJ, Ferris DP. State of the Art and Future Directions for Lower Limb Robotic Exoskeletons. *IEEE Transactions on Neural Systems and Rehabilitation Engineering*. 2017;25(2):171–182. doi:10.1109/TNSRE.2016.2521160.
37. Viteckova S, Kutilek P, Jirina M. Wearable lower limb robotics: A review. *Biocybernetics and Biomedical Engineering*. 2013;33(2):96 – 105. doi:<https://doi.org/10.1016/j.bbe.2013.03.005>.
38. Yan T, Cempini M, Oddo CM, Vitiello N. Review of assistive strategies in powered lower-limb orthoses and exoskeletons. *Robotics and Autonomous Systems*. 2015;64:120 – 136. doi:<https://doi.org/10.1016/j.robot.2014.09.032>.
39. Huo W, Mohammed S, Moreno JC, Amirat Y. Lower Limb Wearable Robots for Assistance and Rehabilitation: A State of the Art. *IEEE Systems Journal*. 2016;10(3):1068–1081. doi:10.1109/JSYST.2014.2351491.
40. Malcolm P, Derave W, Galle S, De Clercq D. A Simple Exoskeleton That Assists Plantarflexion Can Reduce the Metabolic Cost of Human Walking. *PLOS ONE*. 2013;8(2):1–7. doi:10.1371/journal.pone.0056137.
41. Mooney LM, Rouse EJ, Herr HM. Autonomous exoskeleton reduces metabolic cost of human walking during load carriage. *Journal of NeuroEngineering and Rehabilitation*. 2014;11(1):80. doi:10.1186/1743-0003-11-80.
42. Collins SH, Wiggin MB, Sawicki GS. Reducing the energy cost of human walking using an unpowered exoskeleton. *Nature*. 2015;522:212 EP –.
43. Awad LN, Bae J, O'Donnell K, De Rossi SMM, Hendron K, Sloot LH, et al. A soft robotic exosuit improves walking in patients after stroke. *Science Translational Medicine*. 2017;9(400). doi:10.1126/scitranslmed.aai9084.
44. Shamaei K, Cenciarini M, Adams AA, Gregorczyk KN, Schiffman JM, Dollar AM. Biomechanical Effects of Stiffness in Parallel With the Knee Joint During Walking. *IEEE Transactions on Biomedical Engineering*. 2015;62(10):2389–2401. doi:10.1109/TBME.2015.2428636.
45. BROWNING RC, MODICA JR, KRAM R, GOSWAMI A. The Effects of Adding Mass to the Legs on the Energetics and Biomechanics of Walking. *Medicine & Science in Sports & Exercise*. 2007;39(3).
46. Nasiri R, Ahmadi A, Ahmadabadi MN. Reducing the Energy Cost of Human Running Using an Unpowered Exoskeleton. *IEEE Transactions on Neural Systems and Rehabilitation Engineering*. 2018;26(10):2026–2032. doi:10.1109/TNSRE.2018.2872889.
47. Ding Y, Galiana I, Asbeck AT, De Rossi SMM, Bae J, Santos TRT, et al. Biomechanical and Physiological Evaluation of Multi-Joint Assistance With Soft Exosuits. *IEEE Transactions on Neural Systems and Rehabilitation Engineering*. 2017;25(2):119–130. doi:10.1109/TNSRE.2016.2523250.

48. Rosendo A, Iida F. Energy efficient hopping with Hill-type muscle properties on segmented legs. *Bioinspiration & Biomimetics*. 2016;11(3):036002. doi:10.1088/1748-3190/11/3/036002.
49. WVD. Human-exoskeleton interaction. TU Delft; 2015. Available from: <https://doi.org/10.4233/uuid:8cf37c65-a48c-476e-8dcc-eb97c06c26d9>.
50. Buschmann T, Ewald A, von Twickel A, Büschges A. Controlling legs for locomotion—insights from robotics and neurobiology. *Bioinspiration & Biomimetics*. 2015;10(4):041001. doi:10.1088/1748-3190/10/4/041001.
51. Schenau GJVI. From rotation to translation: Constraints on multi-joint movements and the unique action of bi-articular muscles. *Human Movement Science*. 1989;8(4):301 – 337. doi:[https://doi.org/10.1016/0167-9457\(89\)90037-7](https://doi.org/10.1016/0167-9457(89)90037-7).
52. Jacobs R, Bobbert MF, van Ingen Schenau GJ. Mechanical output from individual muscles during explosive leg extensions: The role of biarticular muscles. *Journal of Biomechanics*. 1996;29(4):513 – 523. doi:[https://doi.org/10.1016/0021-9290\(95\)00067-4](https://doi.org/10.1016/0021-9290(95)00067-4).
53. Junius K, Moltedo M, Cherelle P, Rodriguez-Guerrero C, Vanderborght B, Lefever D. Biarticular elements as a contributor to energy efficiency: biomechanical review and application in bio-inspired robotics. *Bioinspiration & Biomimetics*. 2017;12(6):061001. doi:10.1088/1748-3190/aa806e.
54. Prilutsky BI, Zatsiorsky VM. Optimization-Based Models of Muscle Coordination. *Exercise and Sport Sciences Reviews*. 2002;30(1):32–38.
55. van Leeuwen J, Aerts P, Pandy MG. Simple and complex models for studying muscle function in walking. *Philosophical Transactions of the Royal Society of London Series B: Biological Sciences*. 2003;358(1437):1501–1509. doi:10.1098/rstb.2003.1338.
56. Anderson FC, Pandy MG. Dynamic Optimization of Human Walking. *Journal of Biomechanical Engineering*. 2001;123(5):381–390. doi:10.1115/1.1392310.
57. Schenau GJVI. On the Action of Bi-Articular Muscles, a Review. *Netherlands Journal of Zoology*. 1989;40(3).
58. Landin D, Thompson M, Reid M. Actions of Two Bi-Articular Muscles of the Lower Extremity: A Review. *Journal of Clinical Medicine Research*. 2016;8(7).
59. Voronov AV. The Roles of Monoarticular and Biarticular Muscles of the Lower Limbs in Terrestrial Locomotion. *Human Physiology*. 2004;30(4):476–484. doi:10.1023/B:HUMP.0000036345.33099.4f.
60. van Ingen Schenau GJ, Bobbert MF, van Soest AJ. In: Winters JM, Woo SLY, editors. *The Unique Action of Bi-Articular Muscles in Leg Extensions*. New York, NY: Springer New York; 1990. p. 639–652. Available from: https://doi.org/10.1007/978-1-4613-9030-5_41.
61. Elftman H. The function of muscles in locomotion. *Am J Physiol*. 1939;125. doi:10.1152/ajplegacy.1939.125.2.357.
62. Jacobs R, Bobbert MF, van Ingen Schenau GJ. Mechanical output from individual muscles during explosive leg extensions: The role of biarticular muscles. *Journal of Biomechanics*. 1996;29(4):513 – 523. doi:[https://doi.org/10.1016/0021-9290\(95\)00067-4](https://doi.org/10.1016/0021-9290(95)00067-4).

63. Prilutsky BI, Zatsiorsky VM. Tendon action of two-joint muscles: Transfer of mechanical energy between joints during jumping, landing, and running. *Journal of Biomechanics*. 1994;27(1):25 – 34.
doi:[https://doi.org/10.1016/0021-9290\(94\)90029-9](https://doi.org/10.1016/0021-9290(94)90029-9).
64. Elftman H. THE WORK DONE BY MUSCLES IN RUNNING. *American Journal of Physiology-Legacy Content*. 1940;129(3):672–684.
doi:10.1152/ajplegacy.1940.129.3.672.
65. Prilutsky BI, Petrova LN, Raitsin LM. Comparison of mechanical energy expenditure of joint moments and muscle forces during human locomotion. *Journal of Biomechanics*. 1996;29(4):405 – 415.
doi:[https://doi.org/10.1016/0021-9290\(95\)00083-6](https://doi.org/10.1016/0021-9290(95)00083-6).
66. Wells RP. Mechanical energy costs of human movement: An approach to evaluating the transfer possibilities of two-joint muscles. *Journal of Biomechanics*. 1988;21(11):955 – 964.
doi:[https://doi.org/10.1016/0021-9290\(88\)90134-0](https://doi.org/10.1016/0021-9290(88)90134-0).
67. Cleland J. On the Actions of Muscles passing over more than One Joint. *Journal of anatomy and physiology*. 1867;1(1):85–93.
68. Fenn WO. The Mechanics of Muscular Contraction in Man. *Journal of Applied Physics*. 1938;9(3):165–177. doi:10.1063/1.1710406.
69. English C. Stiffness behaviour in two degree of freedom mechanisms. Carleton University, Ottawa, Ontario; 1999.
70. Hogan N. The mechanics of multi-joint posture and movement control. *Biological Cybernetics*. 1985;52(5):315–331. doi:10.1007/BF00355754.
71. Hogan N. Adaptive control of mechanical impedance by coactivation of antagonist muscles. *IEEE Transactions on Automatic Control*. 1984;29(8):681–690. doi:10.1109/TAC.1984.1103644.
72. Hogan N. In: Winters JM, Woo SLY, editors. *Mechanical Impedance of Single- and Multi-Articular Systems*. New York, NY: Springer New York; 1990. p. 149–164. Available from: https://doi.org/10.1007/978-1-4613-9030-5_9.
73. McIntyre J, Mussa-Ivaldi FA, Bizzi E. The control of stable postures in the multijoint arm. *Experimental Brain Research*. 1996;110(2):248–264.
doi:10.1007/BF00228556.
74. Iida F, Rummel J, Seyfarth A. Bipedal walking and running with spring-like biarticular muscles. *Journal of Biomechanics*. 2008;41(3):656 – 667.
doi:<https://doi.org/10.1016/j.jbiomech.2007.09.033>.
75. Sharbafi MA, Rode C, Kurowski S, Scholz D, Möckel R, Radkhah K, et al. A new biarticular actuator design facilitates control of leg function in BioBiped3. *Bioinspiration & Biomimetics*. 2016;11(4):046003.
doi:10.1088/1748-3190/11/4/046003.
76. Roozing W, Ren Z, Tsagarakis NG. Design of a Novel 3-DoF Leg with Series and Parallel Compliant Actuation for Energy Efficient Articulated Robots. In: 2018 IEEE International Conference on Robotics and Automation (ICRA); 2018. p. 1–8.

77. Höppner H, Wiedmeyer W, van der Smagt P. A new biarticular joint mechanism to extend stiffness ranges. In: 2014 IEEE International Conference on Robotics and Automation (ICRA); 2014. p. 3403–3410.
78. Dean JC, Kuo AD. Elastic coupling of limb joints enables faster bipedal walking. *Journal of The Royal Society Interface*. 2009;6(35):561–573. doi:10.1098/rsif.2008.0415.
79. Eilenberg MF, Kuan JY, Herr H. Development and Evaluation of a Powered Artificial Gastrocnemius for Transtibial Amputee Gait. *Journal of Robotics*. 2018;2018:15.
80. Endo K, Swart E, Herr H. An artificial gastrocnemius for a transtibial prosthesis. In: 2009 Annual International Conference of the IEEE Engineering in Medicine and Biology Society; 2009. p. 5034–5037.
81. Eilenberg MF, Endo K, Herr H. Biomechanic and Energetic Effects of a Quasi-Passive Artificial Gastrocnemius on Transtibial Amputee Gait. *Journal of Robotics*. 2018;2018:12.
82. Flynn L, Geeroms J, Jimenez-Fabian R, Vanderborght B, Vitiello N, Lefebvre D. Ankle-knee prosthesis with active ankle and energy transfer: Development of the CYBERLEGS Alpha-Prosthesis. *Robotics and Autonomous Systems*. 2015;73:4 – 15. doi:<https://doi.org/10.1016/j.robot.2014.12.013>.
83. Eslamy M, Grimmer M, Seyfarth A. Adding passive biarticular spring to active mono-articular foot prosthesis: Effects on power and energy requirement. In: 2014 IEEE-RAS International Conference on Humanoid Robots; 2014. p. 677–684.
84. Panizzolo FA, Galiana I, Asbeck AT, Siviy C, Schmidt K, Holt KG, et al. A biologically-inspired multi-joint soft exosuit that can reduce the energy cost of loaded walking. *Journal of NeuroEngineering and Rehabilitation*. 2016;13(1):43. doi:10.1186/s12984-016-0150-9.
85. Quinlivan BT, Lee S, Malcolm P, Rossi DM, Grimmer M, Siviy C, et al. Assistance magnitude versus metabolic cost reductions for a tethered multiarticular soft exosuit. *Science Robotics*. 2017;2(2). doi:10.1126/scirobotics.aah4416.
86. Wiggin MB, Sawicki GS, Collins SH. An exoskeleton using controlled energy storage and release to aid ankle propulsion. In: 2011 IEEE International Conference on Rehabilitation Robotics; 2011. p. 1–5.
87. Xiong C, Zhou T, Zhou L, Wei T, Chen W. Multi-articular passive exoskeleton for reducing the metabolic cost during human walking. In: 2019 Wearable Robotics Association Conference (WearRAcon); 2019. p. 63–67.
88. Seth A, Hicks JL, Uchida TK, Habib A, Dembia CL, Dunne JJ, et al. OpenSim: Simulating musculoskeletal dynamics and neuromuscular control to study human and animal movement. *PLOS Computational Biology*. 2018;14(7):1–20. doi:10.1371/journal.pcbi.1006223.
89. Selinger J, O'Connor S, Wong J, Donelan JM. Humans Can Continuously Optimize Energetic Cost during Walking. *Current Biology*. 2015;25(18):2452 – 2456. doi:<https://doi.org/10.1016/j.cub.2015.08.016>.

90. Gordon KE, Ferris DP. Learning to walk with a robotic ankle exoskeleton. *Journal of Biomechanics*. 2007;40(12):2636 – 2644. doi:<https://doi.org/10.1016/j.jbiomech.2006.12.006>.
91. Delp SL, Anderson FC, Arnold AS, Loan P, Habib A, John CT, et al. OpenSim: Open-Source Software to Create and Analyze Dynamic Simulations of Movement. *IEEE Transactions on Biomedical Engineering*. 2007;54(11):1940–1950. doi:[10.1109/TBME.2007.901024](https://doi.org/10.1109/TBME.2007.901024).
92. Hicks JL, Uchida TK, Seth A, Rajagopal A, Delp SL. Is My Model Good Enough?: Best Practices for Verification and Validation of Musculoskeletal Models and Simulations of Movement. *Journal of Biomechanical Engineering*. 2015;137(2):020905–020905–24. doi:[10.1115/1.4029304](https://doi.org/10.1115/1.4029304).
93. Dembia CL, Silder A, Uchida TK, Hicks JL, Delp SL. Simulating ideal assistive devices to reduce the metabolic cost of walking with heavy loads. *PLOS ONE*. 2017;12(7):1–25. doi:[10.1371/journal.pone.0180320](https://doi.org/10.1371/journal.pone.0180320).
94. Gordon DFN, Henderson G, Vijayakumar S. Effectively Quantifying the Performance of Lower-Limb Exoskeletons Over a Range of Walking Conditions. *Frontiers in Robotics and AI*. 2018;5:61. doi:[10.3389/frobt.2018.00061](https://doi.org/10.3389/frobt.2018.00061).
95. Ong CF, Hicks JL, Delp SL. Simulation-Based Design for Wearable Robotic Systems: An Optimization Framework for Enhancing a Standing Long Jump. *IEEE Transactions on Biomedical Engineering*. 2016;63(5):894–903. doi:[10.1109/TBME.2015.2463077](https://doi.org/10.1109/TBME.2015.2463077).
96. Dorn TW, Wang JM, Hicks JL, Delp SL. Predictive Simulation Generates Human Adaptations during Loaded and Inclined Walking. *PLOS ONE*. 2015;10(4):1–16. doi:[10.1371/journal.pone.0121407](https://doi.org/10.1371/journal.pone.0121407).
97. Nguyen VQ, Umberger BR, Sup FC. Predictive Simulation of Human Walking Augmented by a Powered Ankle Exoskeleton. In: 2019 IEEE 16th International Conference on Rehabilitation Robotics (ICORR); 2019. p. 53–58.
98. LaPrè AK, Umberger BR, Sup F. Simulation of a powered ankle prosthesis with dynamic joint alignment. In: 2014 36th Annual International Conference of the IEEE Engineering in Medicine and Biology Society; 2014. p. 1618–1621.
99. Zhao J, Berns K, de Souza Baptista R, Bó APL. Design of variable-damping control for prosthetic knee based on a simulated biped. In: 2013 IEEE 13th International Conference on Rehabilitation Robotics (ICORR); 2013. p. 1–6.
100. Handford ML, Srinivasan M. Robotic lower limb prosthesis design through simultaneous computer optimizations of human and prosthesis costs. *Scientific Reports*. 2016;6:19983 EP –.
101. Handford ML, Srinivasan M. Energy-Optimal Human Walking With Feedback-Controlled Robotic Prostheses: A Computational Study. *IEEE Transactions on Neural Systems and Rehabilitation Engineering*. 2018;26(9):1773–1782. doi:[10.1109/TNSRE.2018.2858204](https://doi.org/10.1109/TNSRE.2018.2858204).
102. Sreenivasa M, Millard M, Felis M, Mombaur K, Wolf SI. Optimal Control Based Stiffness Identification of an Ankle-Foot Orthosis Using a Predictive Walking Model. *Frontiers in Computational Neuroscience*. 2017;11:23. doi:[10.3389/fncom.2017.00023](https://doi.org/10.3389/fncom.2017.00023).

103. Fey NP, Klute GK, Neptune RR. Optimization of Prosthetic Foot Stiffness to Reduce Metabolic Cost and Intact Knee Loading During Below-Knee Amputee Walking: A Theoretical Study. *Journal of Biomechanical Engineering*. 2012;134(11). doi:10.1115/1.4007824.
104. Rajagopal A, Dembia CL, DeMers MS, Delp DD, Hicks JL, Delp SL. Full-Body Musculoskeletal Model for Muscle-Driven Simulation of Human Gait. *IEEE Transactions on Biomedical Engineering*. 2016;63(10):2068–2079.
105. Thelen DG, Anderson FC, Delp SL. Generating dynamic simulations of movement using computed muscle control. *Journal of Biomechanics*. 2003;36(3):321 – 328. doi:[https://doi.org/10.1016/S0021-9290\(02\)00432-3](https://doi.org/10.1016/S0021-9290(02)00432-3).
106. UMBERGER BR, GERRITSEN KGM, MARTIN PE. A Model of Human Muscle Energy Expenditure. *Computer Methods in Biomechanics and Biomedical Engineering*. 2003;6(2):99–111. doi:10.1080/1025584031000091678.
107. Uchida TK, Hicks JL, Dembia CL, Delp SL. Stretching Your Energetic Budget: How Tendon Compliance Affects the Metabolic Cost of Running. *PLOS ONE*. 2016;11(3):1–19. doi:10.1371/journal.pone.0150378.
108. Marler R, Arora JS. Survey of multi-objective optimization methods for engineering. *Structural and Multidisciplinary Optimization*. 2004;26:369–395.
109. Unal R, Kiziltas G, Patoglu V. Multi-criteria Design Optimization of Parallel Robots. In: 2008 IEEE Conference on Robotics, Automation and Mechatronics; 2008. p. 112–118.
110. Das I, Dennis J. Normal-Boundary Intersection: A New Method for Generating the Pareto Surface in Nonlinear Multicriteria Optimization Problems. *SIAM Journal on Optimization*. 1998;8(3):631–657. doi:10.1137/S1052623496307510.
111. Huang TwP, Kuo AD. Mechanics and energetics of load carriage during human walking. *Journal of Experimental Biology*. 2014;217(4):605–613. doi:10.1242/jeb.091587.
112. Silder A, Delp SL, Besier T. Men and women adopt similar walking mechanics and muscle activation patterns during load carriage. *Journal of Biomechanics*. 2013;46(14):2522–2528. doi:10.1016/j.jbiomech.2013.06.020.
113. IBM Corp . IBM SPSS Statistics for Windows;. Available from: <https://www.ibm.com/analytics/spss-statistics-software>.
114. Browning RC, Modica JR, Kram R, Goswami A. The effects of adding mass to the legs on the energetics and biomechanics of walking. *Medicine & Science in Sports & Exercise*. 2007;39(3):515–525.
115. Royer TD, Martin PE. Manipulations of leg mass and moment of inertia: effects on energy cost of walking. *Medicine & Science in Sports & Exercise*. 2005;37(4):649–656.
116. Soule RG, Goldman RF. Energy cost of loads carried on the head, hands, or feet. *Journal of Applied Physiology*. 1969;27(5):687–690. doi:10.1152/jappl.1969.27.5.687.
117. [de Leva] P. Adjustments to Zatsiorsky-Seluyanov's segment inertia parameters. *Journal of Biomechanics*. 1996;29(9):1223 – 1230. doi:[https://doi.org/10.1016/S0021-9290\(95\)00178-6](https://doi.org/10.1016/S0021-9290(95)00178-6).

118. Laschowski B, McPhee J, Andrysek J. Lower-Limb Prostheses and Exoskeletons With Energy Regeneration: Mechatronic Design and Optimization Review. *Journal of Mechanisms and Robotics*. 2019;11(4). doi:10.1115/1.4043460.
119. Schertzer E, Riemer R. Harvesting biomechanical energy or carrying batteries? An evaluation method based on a comparison of metabolic power. *Journal of NeuroEngineering and Rehabilitation*. 2015;12(1):1–12. doi:10.1186/s12984-015-0023-7.
120. Riemer R, Shapiro A. Biomechanical energy harvesting from human motion: Theory, state of the art, design guidelines, and future directions. *Journal of NeuroEngineering and Rehabilitation*. 2011;8(1):1–13. doi:10.1186/1743-0003-8-22.
121. Seok S, Wang A, Meng Yee Chuah, Otten D, Lang J, Kim S. Design principles for highly efficient quadrupeds and implementation on the MIT Cheetah robot. In: 2013 IEEE International Conference on Robotics and Automation; 2013. p. 3307–3312.
122. Seok S, Wang A, Chuah MY, Hyun DJ, Lee J, Otten DM, et al. Design Principles for Energy-Efficient Legged Locomotion and Implementation on the MIT Cheetah Robot. *IEEE/ASME Transactions on Mechatronics*. 2015;20(3):1117–1129.
123. Donelan JM, Li Q, Naing V, Hoffer JA, Weber DJ, Kuo AD. Biomechanical Energy Harvesting: Generating Electricity During Walking with Minimal User Effort. *Science*. 2008;319(5864):807–810. doi:10.1126/science.1149860.
124. Aguirre-Ollinger G, Colgate JE, Peshkin MA, Goswami A. Design of an active one-degree-of-freedom lower-limb exoskeleton with inertia compensation. *International Journal of Robotics Research*. 2011;30(4):486–499. doi:10.1177/0278364910385730.
125. Colgate E. In: *The Interaction of Robots with Passive Environments: Application to Force Feedback Control*. Springer-Verlag; 1989.
126. COLGATE JE, HOGAN N. Robust control of dynamically interacting systems. *International Journal of Control*. 1988;48(1):65–88. doi:10.1080/00207178808906161.
127. Sawicki GS, Ferris DP. Mechanics and energetics of level walking with powered ankle exoskeletons. *Journal of Experimental Biology*. 2008;211(9):1402–1413. doi:10.1242/jeb.009241.
128. Torricelli D, Gonzalez J, Weckx M, Jiménez-Fabián R, Vanderborght B, Sartori M, et al. Human-like compliant locomotion: State of the art of robotic implementations. *Bioinspiration and Biomimetics*. 2016;11(5). doi:10.1088/1748-3190/11/5/051002.
129. Jackson RW, Collins SH. An experimental comparison of the relative benefits of work and torque assistance in ankle exoskeletons. *Journal of Applied Physiology*. 2015;119(5):541–557. doi:10.1152/japplphysiol.01133.2014.
130. Lewis CL, Ferris DP. Invariant hip moment pattern while walking with a robotic hip exoskeleton. *Journal of Biomechanics*. 2011;44(5):789 – 793. doi:<https://doi.org/10.1016/j.jbiomech.2011.01.030>.

131. Kao PC, Lewis CL, Ferris DP. Invariant ankle moment patterns when walking with and without a robotic ankle exoskeleton. *Journal of Biomechanics*. 2010;43(2):203 – 209. doi:<https://doi.org/10.1016/j.jbiomech.2009.09.030>.
132. Galle S, Malcolm P, Derave W, Clercq DD. Adaptation to walking with an exoskeleton that assists ankle extension. *Gait & Posture*. 2013;38(3):495 – 499. doi:<https://doi.org/10.1016/j.gaitpost.2013.01.029>.
133. Koller JR, Jacobs DA, Ferris DP, Remy CD. Learning to walk with an adaptive gain proportional myoelectric controller for a robotic ankle exoskeleton. *Journal of NeuroEngineering and Rehabilitation*. 2015;12(1):97. doi:10.1186/s12984-015-0086-5.
134. Lenzi T, Carrozza MC, Agrawal SK. Powered Hip Exoskeletons Can Reduce the User's Hip and Ankle Muscle Activations During Walking. *IEEE Transactions on Neural Systems and Rehabilitation Engineering*. 2013;21(6):938–948. doi:10.1109/TNSRE.2013.2248749.
135. Vanderpool MT, Collins SH, Kuo AD. Ankle fixation need not increase the energetic cost of human walking. *Gait & Posture*. 2008;28(3):427 – 433. doi:<https://doi.org/10.1016/j.gaitpost.2008.01.016>.
136. Cenciarini M, Dollar AM. Biomechanical considerations in the design of lower limb exoskeletons. In: 2011 IEEE International Conference on Rehabilitation Robotics; 2011. p. 1–6.
137. Johnson MA, Polgar J, Weightman D, Appleton D. Data on the distribution of fibre types in thirty-six human muscles: An autopsy study. *Journal of the Neurological Sciences*. 1973;18(1):111 – 129. doi:[https://doi.org/10.1016/0022-510X\(73\)90023-3](https://doi.org/10.1016/0022-510X(73)90023-3).
138. Newham DJ, Mills KR, Quigley BM, Edwards RHT. Pain and Fatigue after Concentric and Eccentric Muscle Contractions. *Clinical Science*. 1983;64(1):55–62. doi:10.1042/cs0640055.
139. Geijtenbeek T. SCONE: Open Source Software for Predictive Simulation of Biological Motion. *Journal of Open Source Software*. 2019;4(38):1421. doi:10.21105/joss.01421.
140. Zhang J, Fiers P, Witte KA, Jackson RW, Poggensee KL, Atkeson CG, et al. Human-in-the-loop optimization of exoskeleton assistance during walking. *Science*. 2017;356(6344):1280–1284. doi:10.1126/science.aal5054.